The Raymond and Beverly Sackler Faculty of Exact Sciences
Tel Aviv University

School of Physics and Astronomy
Department of Condensed Matter Physics

Universal bounds on entropy production inferred from observed statistics

Thesis submitted in partial fulfillment of the requirements for the Master of Sciences degree in the School of Physics and Astronomy, Tel Aviv University

By

Eden Nitzan

The research work for the thesis has been carried out under the supervision of **Dr. Gili Bisker**

Acknowledgements

I would like to thank my thesis supervisor Dr. G. Bisker for her constant support over the last two years. Her belief in me encouraged me to do things I would never think I could do.

I want to express my appreciation to my lab members for being there for me, helping whenever I needed them, and making my time in the lab much more pleasant. A special thanks to Dr. A. Ghosal, who took care of me and helped me personally and professionally more than I would expect her to. I would never have made it without her.

I want to thank my friends and roommates, Mr. T. Schneider and Mr. G. Weizman, for listening to me talking about my work and struggles even when they did not want to.

I want to thank the departmental office staff for their help.

I dedicate this work to my parents, Eyal and Pnina, and my sister Gal. I am very grateful for their support.

Publication

A paper summarizing the results presented in this thesis was submitted for publication [1].

"Universal bounds on entropy production inferred from observed statistics"
Eden Nitzan, Aishani Ghosal, and Gili Bisker
arXiv:2212.01783, 2022

Abstract

Nonequilibrium processes break time-reversal symmetry and generate entropy. Living systems are driven out-of-equilibrium at the microscopic level of molecular motors that exploit chemical potential gradients to transduce free energy to mechanical work, while dissipating energy. The amount of energy dissipation, or the entropy production rate (EPR), sets thermodynamic constraints on cellular processes. Practically, calculating the total EPR in experimental systems is challenging due to the limited spatiotemporal resolution and the lack of complete information on every degree of freedom. Here, we propose a new inference approach for a tight lower bound on the total EPR given partial information, based on an optimization scheme that uses the observed transitions and waiting times statistics. We introduce hierarchical bounds relying on the first- and second-order transitions, and the moments of the observed waiting time distributions, and apply our approach to two generic systems of a hidden network and a molecular motor, with lumped states. Finally, we show that a lower bound on the total EPR can be obtained even when assuming a simpler network topology of the full system.

Contents

1

Introduction

1.1 Overview

Advances in experimental techniques over the last few decades have opened new possibilities for studying systems at the single-molecule level [2–4]. In parallel, new theoretical approaches of stochastic thermodynamics for studying the physics of nonequilibrium, small fluctuating systems have emerged [5–7]. These include the mathematical relations describing symmetry properties of the stochastic quantities like work [8–10] heat [10, 11], and entropy production [12, 13], leading to fundamental limits on physical systems like heat engines [14–16] refrigerators [17], and biological processes [18, 19].

Living systems operate far-from-equilibrium and constantly produce entropy. At the molecular level, the hydrolysis of fuel molecules, such as Adenosine triphosphate (ATP), powers nonequilibrium cellular processes, utilizing part of the liberated free energy for physical work, while the rest is dissipated [6]. The dissipation, or entropy production, is a signature of irreversible processes and can be used as a direct measure of the deviation from thermal equilibrium [20–23]. Therefore, the entropy production rate plays an important role in our understanding of the physics and underlying mechanism, governing biological and chemical processes [14–16, 18, 19, 24].

Various studies have focused on estimating the mean entropy production rate using the thermodynamic uncertainty relations (TUR) using current fluctuations [25–30], fluctuations of first passage time [31, 32], kinetic uncertainty relation in terms of the activity [33], or unified thermodynamic and kinetic uncertainty relations [34]. Other approaches utilize waiting-time distributions [35–37], machine learning [38–41], and single trajectory data [42–44]. Additional studies calculate higher moments of the full probability density function of the entropy production [45], use irreversible currents in stochastic dynamics described by a set of Langevin equations [46], or linear response theory [24].

Estimating the total EPR is only possible if we have knowledge regarding all of the degrees of freedom that are out-of-equilibrium [47, 48]. However, due to practical limitations on the spatiotemporal resolution, not all of them can be experimentally accessible, and one can only obtain a lower bound on the total EPR for partially observed or coarse-grained systems [49–55].

The passive partial entropy production rate, $\sigma_{\rm pp}$, is an estimator for the EPR calculated from the transitions between two observed states, which bounds the total EPR [49, 56–58]. This estimator, however, fails to provide a non-zero bound in case of vanishing current over the observed link, *i.e.*, at stalling conditions [49]. Other EPR estimators for partially observed systems based on inequality relations like the TUR [25–27, 33, 34] also fail to provide a non-trivial bound on the total EPR in the absence of net flux in the system.

The Kullback-Leibler Divergence (KLD) estimator, $\sigma_{\rm KLD}$, is based on the KLD, or the relative entropy, between the time-forward and the time-revered path probabilities [22, 47, 59–63]. For semi-Markov processes, this estimator is a sum of two contributions. The first stems from transitions irreversibility or cycle affinities, $\sigma_{\rm aff}$, whereas the second stems from broken time-reversal symmetry reflected in irreversibility in waiting time distributions (WTD), $\sigma_{\rm WTD}$ [64]. Using the KLD estimator, one can obtain a non-trivial lower bound on the total EPR for second-order semi-Markov processes even in the absence of the net current [36, 64–66]. Moreover, a lower bound on the total EPR can be obtained from the KLD between

transition-based WTD [60, 65, 67].

Recently developed estimators solved an optimization problem to obtain a lower bound on the entropy production. For a discrete-time model, Ehrich proposed to search over the possible underlying systems that maintain the same observed statistics using knowledge on the number of hidden states [68]. For continuous-time models, Skinner and Dunkel minimized the EPR on a canonical form of the system that preserved the first- and second-order transition statistics to yield a lower bound on the total EPR, σ_2 [69]. The authors also formulated an optimization problem to infer the EPR in a system with two observed states using the waiting time statistics [35].

In this thesis, we provide a tight bound on the total EPR by formulating an optimization problem based on the statistics of both transitions and waiting times. For a system with a known topology (i.e. the number of states and possible transitions), we calculate the analytical expressions of the statistics as functions of the transition rates and the steady-state probabilities, which describe a possible underlying system and are used as variables in the optimization problem. These analytical expressions are then used to constrain the optimization variables to match the observed statistics. We show for a few continuous-time Markov chain systems that for the waiting-time statistics using only the first moment of the WTD already provides close-to-total EPR value. Our approach outperforms other estimators, such as σ_{pp}, σ_{KLD}, σ_{aff}, and σ_2, in terms of the tightness of the lower bound. In the case of a complex model, where the formulation of the optimization problem might not be practical due to the number of constraints, or in case the full topology is not known, we show numerically that assuming a simpler underlying topology can provide a lower bound on the total EPR.

1.2 Model

We assume a continuous time Markov chain over a finite and discrete set of states $i = \{1, 2, \ldots, N\}$. A trajectory is described by a sequence of states and their corresponding residence times before a transition to the next state occurs. Being a Markovian process, the jump probabilities depend only on the current state.

The transition rates w_{ij} from state i to j determine the time evolution of the probabilities for the system to be in each state, according to the master equation $\frac{d}{dt}\boldsymbol{p}(t)^T = \boldsymbol{p}(t)^T\boldsymbol{W}$, where T is the transpose operator, and $\boldsymbol{W}$ is the rate matrix

$$[\boldsymbol{W}]_{ij} = \begin{cases} w_{ij} & j \neq i \\ -\lambda_i & j = i \end{cases} \tag{1.1}$$

$\boldsymbol{p}(t)$ is a column vector of the state probabilities at time t, with $\sum_i p_i(t) = 1$, and the diagonal entries are calculated according to $\lambda_i = \sum_{j\neq i} w_{ij}$ for probability conservation.

At the long-time limit, the system eventually reaches a steady state $\boldsymbol{\pi}$, where $\lim_{t\to\infty} p_i(t) = \pi_i$ such that $0 = \frac{d}{dt}\boldsymbol{\pi}^T = \boldsymbol{\pi}^T\boldsymbol{W}$ [70].

The waiting time at each state i is an exponential random variable with mean waiting time of $\tau_i = \lambda_i^{-1}$.

The mass rates n_{ij} (i.e. the rate to observe the transition $i \to j$) are defined as follows:

$$n_{ij} = \begin{cases} \pi_i w_{ij} & j \neq i \\ 0 & j = i \end{cases} \tag{1.2}$$

From the master equation, we can easily see that a "mass" conservation equation is satisfied $\sum_j n_{ij} = \sum_j n_{ji}$ (the rate to observe any transition to state i must be equal to the rate to observe any transition from i). Thus the name "mass rates".

The transition probabilities from state i to state j can be written in terms of the mass rates:

$$p_{ij} = \frac{w_{ij}}{\lambda_i} = \frac{n_{ij}}{\sum_{j'\neq i} n_{ij'}} \tag{1.3}$$

The steady-state total EPR can be calculated by multiplying the net currents and the mass rate ratios (affinities), summing over all the links [6, 7]:

$$\begin{aligned}\sigma_{\text{tot}} &= \sum_{i,j} \pi_i w_{ij} \log\left(\frac{\pi_i w_{ij}}{\pi_j w_{ji}}\right) \\ &= \sum_{i,j} n_{ij} \log\left(\frac{n_{ij}}{n_{ji}}\right) \\ &= \sum_{i<j} (n_{ij} - n_{ji}) \log\left(\frac{n_{ij}}{n_{ji}}\right)\end{aligned} \tag{1.4}$$

Where $n_{ij} - n_{ji}$ is the net current and $\log\left(\frac{\pi_i w_{ij}}{\pi_j w_{ji}}\right)$ is the affinity, for the link i to j.

Given a long trajectory of a total duration T, the steady-state probability π_i is the fraction of time spent in state i, and the mass rate n_{ij} is the number of transitions $i \to j$ divided by T.

According to the definition of the mass rates in Eq. 1.2, at the steady state, mass conservation is satisfied at each state:

$$\forall_i : \sum_j n_{ij} = \sum_j n_{ji} \tag{1.5}$$

In many practical scenarios, some of the microstates cannot be distinguished, and the transitions between them cannot be observed. In such a case, a set of states $\{i_1, i_2, \ldots, i_{N_I}\}$ is observed as a single coarse-grained state I (Fig. 1.1(a)). The observed trajectory, therefore, includes only coarse-grained states and the combined residence time (Fig. 1.1(b)), and it is not necessarily a Markovian process [64]. Such a decimation procedure of lumping several states can give rise to semi-Markovian processes of any order depending on the topology of the network [69, 71–73]. In this case, the observed statistics of two or more consecutive transitions may give us additional information on the process.

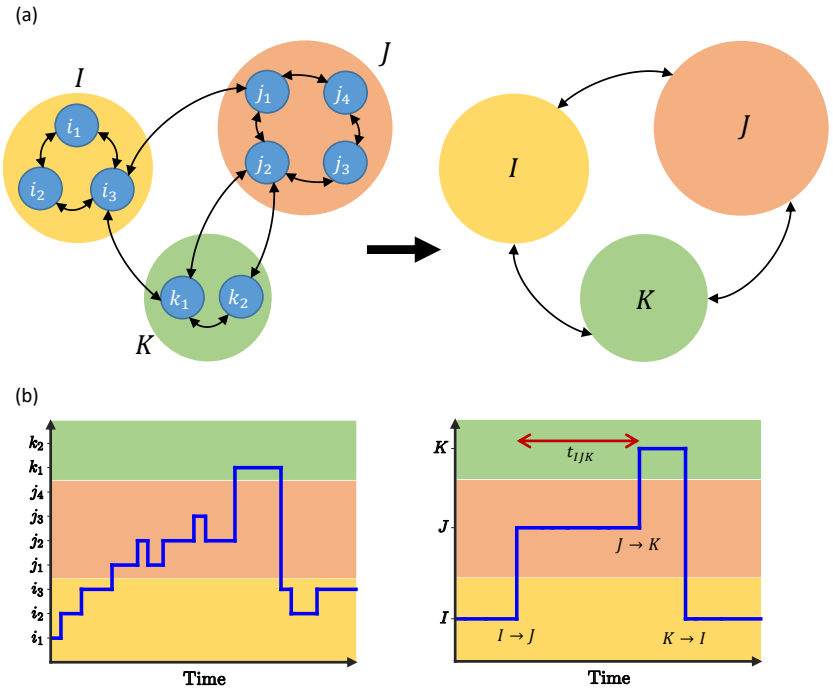

Figure 1.1: Coarse graining. (a) The full Markovian system (left) and the coarse-grained system (right). (b) An example for a full trajectory (left) containing the actual states and the corresponding coarse-grained trajectory (right) containing only the observed states.

1.3 Entropy production rate and irreversibility

This section presents the relation between EPR and irreversibility.

1.3.1 Irreversibility

For fixed observation time T, we denote a trajectory $\gamma_T = \{(i_0, t_0), \ldots, (i_N, t_N)\}$, which is a chronological sequence of states $(i_0, \ldots, i_N\}$ and waiting times $\{t_0, \ldots, t_N\}$, and $\sum_i t_i = T$. The time reversed trajectory is denoted by $\tilde{\gamma_T} = \{(i_N, t_N), \ldots, (i_0, t_0)\}$.

As mentioned in section 1.2, the waiting time distribution is an exponential distribution with mean of $1/\lambda$, together with the jump probabilities, p_{ij}, we get the joint probability for transition and waiting time:

$$\psi_{ij}(t) = w_{ij} e^{-\lambda_i t} \tag{1.6}$$

Thus, the probability to observe the trajectory γ is:

$$\mathcal{P}(\gamma_T) = e^{-t_N \lambda_{i_N}} \prod_{n=0}^{N-1} [w_{i_n, i_{n+1}} e^{-t_n \lambda_{i_n}}] \pi_{i_0} \tag{1.7}$$

where the initial state i_0 is sampled from the steady-state probabilities $\boldsymbol{\pi}$. Now we construct a trajectory observable:

$$\mathcal{R}[\gamma_T] \equiv \log \left(\frac{\mathcal{P}[\gamma_T]}{\mathcal{P}[\tilde{\gamma}_T]} \right) \tag{1.8}$$

where $\mathcal{P}[\tilde{\gamma_T}]$ is the probability to observe the reversed trajectory $\tilde{\gamma_T}$.

After plugging Eq. 1.7 into Eq. 1.8:

$$\begin{aligned} \mathcal{R}[\gamma_T] &= \log \left(\frac{\pi_{i_0}}{\pi_{i_N}} \right) + \sum_{n=0}^{N-1} \log \left(\frac{w_{i_n, i_{n+1}}}{w_{i_{n+1}, i_n}} \right) \\ &= \log \left(\frac{\pi_{i_0}}{\pi_{i_N}} \right) + \sum_{i,j} \phi_{ij} \log \left(\frac{w_{ij}}{w_{ji}} \right) \end{aligned} \tag{1.9}$$

where ϕ_{ij} is the number of transitions $i \to j$ in the trajectory γ:

$$\phi_{ij} = \sum_{n=0}^{N-1} \delta_{i, i_n} \delta_{j, i_{n+1}} \tag{1.10}$$

The long-time average yields:

$$\begin{aligned}\lim_{T\to\infty}\langle\mathcal{R}[\gamma_T]\rangle/T &= \lim_{T\to\infty}\left[\frac{\log\left(\frac{\pi_{i_0}}{\pi_{i_N}}\right)}{T}+\sum_{i,j}\frac{\phi_{ij}}{T}\log\left(\frac{w_{ij}}{w_{ji}}\right)\right]\\ &= 0+\sum_{i,j}n_{ij}\log\left(\frac{w_{ij}}{w_{ji}}\right)\\ &= \sum_{i,j}n_{ij}\log\left(\frac{w_{ij}}{w_{ji}}\right)+\sum_{i,j}n_{ij}\log\left(\frac{\pi_i}{\pi_j}\right)\\ &= \sum_{i,j}n_{ij}\log\left(\frac{\pi_i w_{ij}}{\pi_j w_{ji}}\right)\\ &= \sum_{i<j}(n_{ij}-n_{ji})\log\left(\frac{n_{ij}}{n_{ji}}\right)\end{aligned} \tag{1.11}$$

Notice that by definition $n_{ij}=\lim_{T\to\infty}\phi_{ij}/T$. In addition, we used $\sum_{i,j}n_{ij}\log\left(\frac{\pi_i}{\pi_j}\right)=0$:

$$\begin{aligned}\sum_{i,j}n_{ij}\log\left(\frac{\pi_i}{\pi_j}\right) &= \sum_{i,j}\pi_i w_{ij}\log(\pi_i)-\sum_{i,j}\pi_i w_{ij}\log(\pi_j)\\ &= \sum_{i\neq j}\pi_i w_{ij}\log(\pi_i)-\sum_{i\neq j}\pi_i w_{ij}\log(\pi_j)+\left[\pi_i[\boldsymbol{W}]_{ii}\log(\pi_i)-\pi_i\left[\boldsymbol{W}\right]_{ii}\log(\pi_i)\right]\\ &= \sum_{i,j}\pi_i[\boldsymbol{W}]_{ij}\log(\pi_i)-\sum_{i,j}\pi_i[\boldsymbol{W}]_{ij}\log(\pi_j)\\ &= \sum_i\pi_i(\sum_j[\boldsymbol{W}]_{ij})\log(\pi_i)-\sum_j(\sum_i\pi_i[\boldsymbol{W}]_{ij})\log(\pi_j)\end{aligned} \tag{1.12}$$

By the definition of the rate matrix $\forall_i:\ \sum_j[\boldsymbol{W}]_{ij}=0$ and from the master equation at the steady state $\forall_j:\ 0=\frac{d\pi_j}{dt}=\sum_i\pi_i[\boldsymbol{W}]_{ij}$.
Thus, we justified $\sum_{i,j}n_{ij}\log\left(\frac{\pi_i}{\pi_j}\right)=0$.

To quantify the time irreversibility we use the Kullback-Leibler divergence between the probability to observe the trajectory forward in time and the probability to observe the reversed trajectory:

$$\begin{aligned}\mathcal{D}[\mathcal{P}[\gamma_T]||\mathcal{P}[\tilde{\gamma}_T]] &= \int_{\gamma_T}\mathcal{P}[\gamma_T]\log\left(\frac{\mathcal{P}[\gamma_T]}{\mathcal{P}[\tilde{\gamma}_T]}\right)\\ &= \langle\log\left(\frac{\mathcal{P}[\gamma_T]}{\mathcal{P}[\tilde{\gamma}_T]}\right)\rangle=\langle\mathcal{R}[\gamma_T]\rangle\end{aligned} \tag{1.13}$$

To conclude, from Eq. 1.11 and Eq. 1.13:

$$\lim_{T\to\infty}\frac{1}{T}\mathcal{D}[\mathcal{P}[\gamma_T]||\mathcal{P}[\tilde{\gamma}_T]] = \sum_{i<j}(n_{ij}-n_{ji})\log\left(\frac{n_{ij}}{n_{ji}}\right) \tag{1.14}$$

1.3.2 Entropy production rate

We look at the ensemble-averaged entropy which depend on the state probabilities of the system, p_i.

$$S = -k_B\sum_i p_i\log(p_i) \tag{1.15}$$

Now we take a derivative by time.

$$\begin{aligned}\frac{dS}{dt} &= -k_B\sum_i\left[\frac{dp_i}{dt}\log(p_i)+p_i\frac{1}{p_i}\frac{dp_i}{dt}\right] = -k_B\sum_i\frac{dp_i}{dt}\log(p_i) - k_B\sum_i\frac{dp_i}{dt}\\ &= -k_B\sum_i\frac{dp_i}{dt}\log(p_i) - k_B\frac{d(\sum_i p_i)}{dt} = -k_B\sum_i\frac{dp_i}{dt}\log(p_i) - k_B\frac{d(1)}{dt}\\ &= -k_B\sum_i\frac{dp_i}{dt}\log(p_i)\end{aligned} \tag{1.16}$$

Using the Markovian master equation:

$$\frac{dp_i}{dt}(t) = \sum_j p_j(t)[\mathbf{W}]_{ji} \tag{1.17}$$

We get:

$$\frac{dS}{dt} = -k_B\sum_i\frac{dp_i}{dt}\log(p_i) = -k_B\sum_{i,j}p_j[\mathbf{W}]_{ji}\log(p_i) \tag{1.18}$$

By the definition of the rate matrix $\mathbf{W}$:

$$\forall_j:\ \sum_i[\mathbf{W}]_{ji} = 0 \tag{1.19}$$

Thus:

$$\begin{aligned}
\frac{dS}{dt} &= -k_B \sum_{i,j} p_j [\mathbf{W}]_{ji} \log(p_i) \\
&= -k_B \sum_{i,j} p_j [\mathbf{W}]_{ji} \log(p_i) + k_B \sum_j p_j \left(\sum_i [\mathbf{W}]_{ji} \right) \log(p_j) \\
&= -k_B \sum_{i,j} p_j [\mathbf{W}]_{ji} \log(p_i) + k_B \sum_{i,j} p_j [\mathbf{W}]_{ji} \log(p_j) \\
&= -k_B \sum_{i,j} p_j [\mathbf{W}]_{ji} \log\left(\frac{p_i}{p_j}\right) \\
&= \frac{k_B}{2} \sum_{i,j} (p_i [\mathbf{W}]_{ij} - p_j [\mathbf{W}]_{ji}) \log\left(\frac{p_i}{p_j}\right) \\
&= \frac{k_B}{2} \sum_{i,j} (p_i [\mathbf{W}]_{ij} - p_j [\mathbf{W}]_{ji}) \log\left(\frac{p_i [\mathbf{W}]_{ij}}{p_j [\mathbf{W}]_{ji}}\right) + \frac{k_B}{2} \sum_{i,j} (p_i [\mathbf{W}]_{ij} - p_j [\mathbf{W}]_{ji}) \log\left(\frac{[\mathbf{W}]_{ji}}{[\mathbf{W}]_{ij}}\right) \\
&\equiv \sigma_{\text{tot}} + \dot{S}_e
\end{aligned} \tag{1.20}$$

Where:
$\sigma_{\text{tot}} = \frac{k_B}{2} \sum_{i,j} (p_i [\mathbf{W}]_{ij} - p_j [\mathbf{W}]_{ji}) \log\left(\frac{p_i [\mathbf{W}]_{ij}}{p_j [\mathbf{W}]_{ji}}\right)$ is the entropy production rate.
$\dot{S}_e = \frac{k_B}{2} \sum_{i,j} (p_i [\mathbf{W}]_{ij} - p_j [\mathbf{W}]_{ji}) \log\left(\frac{[\mathbf{W}]_{ji}}{[\mathbf{W}]_{ij}}\right)$ is the entropy flow.

Therefore, we got the expression for the steady-state entropy production rate (setting $k_B = 1$ and $p_i = \pi_i$):

$$\begin{aligned}
\sigma_{\text{tot}} &= \sum_{i<j} (\pi_i w_{ij} - \pi_j w_{ji}) \log\left(\frac{\pi_i w_{ij}}{\pi_j w_{ji}}\right) \\
&= \sum_{i<j} (n_{ij} - n_{ji}) \log\left(\frac{n_{ij}}{n_{ji}}\right)
\end{aligned} \tag{1.21}$$

Which bring us to the relation between EPR to irreversibility. Eq. 1.14 from the previous section together with Eq. 1.21 from this section, gives us:

$$\sigma_{\text{tot}} = \lim_{T \to \infty} \frac{1}{T} \mathcal{D}[\mathcal{P}[\gamma_T] || \mathcal{P}[\tilde{\gamma}_T]] \tag{1.22}$$

Therefore, EPR can be used to quantify the irreversibility of a process.

1.4 Passive partial production rate

The passive partial entropy production rate, $\sigma_{\rm pp}$, is an estimator for the EPR calculated from the transitions between two observed states, which bounds the total EPR [49, 56–58]. Suppose we observe only two states i' and j', which are Markovian, and the transitions between them. Thus, we can calculate the transition mass rates $n_{i'j'}$ and $n_{j'i'}$ in order to calculate the entropy production inferred from the transitions between them:

$$\sigma_{\rm pp} = (n_{i'j'} - n_{j'i'}) \log(\frac{n_{i'j'}}{n_{j'i'}}) \tag{1.23}$$

We can easily see that σ_{pp} is a lower bound for the total entropy production:

$$\begin{aligned}
\sigma_{tot} &= \sum_{i<j} (n_{ij} - n_{ji}) \log(\frac{n_{ij}}{n_{ji}}) \\
&= (n_{i'j'} - n_{j'i'}) \log(\frac{n_{i'j'}}{n_{j'i'}}) + \sum_{\substack{i<j \\ (i,j)\neq(i',j')}} (n_{ij} - n_{ji}) \log(\frac{n_{ij}}{n_{ji}}) \\
&\geq (n_{i'j'} - n_{j'i'}) \log(\frac{n_{i'j'}}{n_{j'i'}}) = \sigma_{pp}
\end{aligned}$$

This estimator, however, fails to provide a non-zero bound in case of vanishing current over the observed link, *i.e.*, at stalling conditions [49]. Other EPR estimators for partially observed systems based on inequality relations like the TUR [25–27, 33, 34] also fail to provide a non-trivial bound on the total EPR in the absence of net flux in the system.

1.5 KLD estimator

The Kullback-Leibler Divergence (KLD) estimator, $\sigma_{\rm KLD}$, is based on the KLD, or the relative entropy, between the time-forward and the time-revered path probabilities [22, 47, 59–63]. For semi-Markov processes, this estimator is a sum of two contributions. The first stems from transitions irreversibility or cycle affinities, $\sigma_{\rm aff}$, whereas the second stems from broken time-reversal symmetry reflected in irreversibility in waiting time distributions (WTD), $\sigma_{\rm WTD}$ [64].

For this estimator, they consider statistics based on second-order transitions. We take into account the former observed state in addition to the current one. We use a new description where a state in our trajectory consists of the former state I and the current one J. Thus, a state in our new trajectory is described as $[IJ]$. Then, we calculate the KLD bwtween the forward and backward path probabilities based on this description.

$$\begin{aligned}\sigma_{\mathrm{KLD}} &= \sigma_{\mathrm{aff}} + \sigma_{\mathrm{WTD}} \\ &= \frac{1}{\mathcal{T}} \sum_{I,J,K} p_{IJK} \log \left(\frac{p([IJ] \to [JK])}{p([KJ] \to [JI])} \right) \\ &+ \frac{1}{\mathcal{T}} \sum_{I,J,K} p_{IJK} D\left[\psi_{IJK}(t) || \psi_{KJI}(t)\right]\end{aligned} \tag{1.24}$$

where $p([IJ] \to [JK])$ is the probability to observe the transition $J \to K$ given the previous transition was $I \to J$, p_{IJK} is the probability to observe the second-order transition $I \to J \to K$, and $D[p||q]$ is the KLD between the probability distributions p and q.

Using the KLD estimator, one can obtain a non-trivial lower bound on the total EPR for second-order semi-Markov processes even in the absence of observed net current [36, 64–66, 74]. Moreover, a lower bound on the total EPR can be obtained from the KLD between transition-based WTD [60, 65, 67].

1.6 Optimization based estimators

Recently developed estimators solved an optimization problem to obtain a lower bound on the entropy production.

1.6.1 σ_{fit} estimator

For a discrete-time model, Ehrich proposed to search over the possible underlying systems that maintain the same observed statistics using knowledge on the number of hidden states [68]. The optimization problem is formulated on a specific system

of four states with two observed states and two states coarse-grained as one. A similar formulation can be applied on similar systems as long as the number of the observed states is equal to the number of hidden states and the matrices of jump probabilities can be inverted.

1.6.2 σ_2 estimator

For continuous-time models, Skinner and Dunkel minimized the EPR on a canonical form of the system that preserved the first- and second-order transition statistics to yield a lower bound on the total EPR, σ_2 [69]. The canonical form can be reached by applying a few steps which changes the underlying system and each step is shown to not raise the EPR while keeping the first and second-order mass rate statistics. Furthermore, they showed that for each 3 coarse-grained states $\{I, J, K\}$, the number of inner states of J in the canonical form, which are connected to I and K, is at most four in order to get the minimum EPR. Since the canonical form has a simple topology we can easily get the constraints for the optimization problem, which make sure the observed statistics are conserved.

1.6.3 σ_T estimator

Skinner and Dunkel also formulated an optimization problem to infer the EPR in a system with two observed states using the waiting time statistics [35]. With a simple re-scaling to the rates and steady-state probabilities of the underlying system, they show you can get an estimator which equals to a factor $\frac{2k_B}{\langle t_A \rangle + \langle t_B \rangle}$ multiplied by the value of a function Λ which depends only on the ratio $\frac{\text{Var } t_A}{\langle t_A \rangle^2}$, where t_A and t_B represent the waiting times in each of the observed states. The function Λ can be computed numerically, by solving an optimization problem, for each value of $\frac{\text{Var } t_A}{\langle t_A \rangle^2}$.

2

Method

Can we find a better estimator which outperforms the previous ones?
In order to achieve that, we introduce a novel method, which utilizes additional information that was not considered in previous works. This information is the underlying system topology.

2.1 Bounding the entropy production rate

Given a coarse-grained system with a model of the full underlying Markovian network topology, we can formulate an optimization problem for obtaining a tight bound on the total EPR. We consider a few observables: the coarse-grained steady-state probabilities, π_I, which is the probability of observing the system in the coarse-grained state I; the first-order mass rates, n_{IJ}, which is the rate of observing the transition $I \to J$; the second order mass rates, n_{IJK}, which is the rate of observing the transition $I \to J$ followed by the transition $J \to K$; and the conditional waiting time distributions $\psi_{IJK}(t)$, which is the distribution of waiting times in a coarse-grained state J before a transition to a coarse-grained state K occurs, conditioned on the previous transition being $I \to J$.

We search over the space of all possible underlying systems with the same topology as our hypothesized Markovian model that give rise to the same observed statis-

tics, while minimizing the EPR. Trivially, the EPR of the coarse-grained system at hand is bounded from below by the EPR of the underlying Markovian system with the same observed statistics after coarse-graining, having the minimal value of entropy production.

2.1.1 Analytical expressions of the observed statistics

The observed statistics of the coarse-grained system can be expressed analytically in terms of the mass rates and steady-state probabilities of the model underlying system. From probability and mass conservation, $\pi_I = \sum_{i\in I} \pi_i$, and $n_{IJ} = \sum_{i\in I, j\in J} n_{ij}$, respectively. The mass conservation for the second-order transitions n_{IJK} must include all the paths starting at state $i \in I$, passing through a state in J, where any number of transitions might occur inside J, and jumping to state $k \in K$. To account for the transitions within J, we define the matrix $\boldsymbol{P}_{JJ}$ of the transition probabilities between states in J, $j_m, j_n \in J$:

$$[\boldsymbol{P}_{JJ}]_{mn} = \begin{cases} p_{j_m j_n} & m \neq n \\ 0 & m = n \end{cases} \tag{2.1}$$

Summing over the possible transitions from I, transitions within J, and transitions to K, we have (see Appendix A):

$$n_{IJK} = \sum_{i\in I, k\in K} \boldsymbol{n}_{iJ}^T [\mathbb{I} - \boldsymbol{P}_{JJ}]^{-1} \boldsymbol{p}_{Jk} \tag{2.2}$$

where $\mathbb{I}$ is the identity matrix of the size of $\boldsymbol{P}_{JJ}$, and $\boldsymbol{n}_{iJ}$ and $\boldsymbol{p}_{Jk}$ are column vectors of the mass rates from state $i \in I$ to any state $j \in J$, and jump probabilities from any state $j \in J$ to a state $k \in K$, respectively:

$$\boldsymbol{n}_{iJ}^T = [n_{ij_1}, n_{ij_2}, \cdots, n_{ij_{N_J}}] \tag{2.3}$$

and:

$$\boldsymbol{p}_{Jk}^T = [p_{j_1 k}, p_{j_2 k}, \cdots, p_{j_{N_J} k}] \tag{2.4}$$

The conditional waiting time distribution $\psi_{IJK}(t)$ can be calculated by the Laplace and inverse-Laplace transforms (full derivations can be found in Appendix B).

We start from the Laplace transform of $\psi_{ij}(t) = w_{ij}e^{-\lambda_i t}$, the joint probability distribution of the transition $i \to j$ and the waiting time in the Markovian state i:

$$\tilde{\psi}_{ij}(s) = \mathcal{L}\{\psi_{ij}(t)\} = \int_0^\infty \psi_{ij}(t)e^{-ts}dt = \frac{w_{ij}}{s+\lambda_i} \tag{2.5}$$

Note that for any function $f(t)$, $\tilde{f}(s \to 0) = \int_0^\infty f(t)e^{-ts}dt|_{s\to 0} = \int_0^\infty f(t)dt$ is the normalization of $f(t)$. Here, $\psi_{ij}(t)$ is normalized to p_{ij}, *i.e.*, $p_{ij} = \int_0^\infty \psi_{ij}(t)dt$ (Eq. 1.3).

Now, we consider the simple case where the second-order transition through the coarse-grained state J starts and ends in specific Markovian states $i \in I$ and $k \in K$, respectively. The Laplace transform of the distribution of waiting times in J before a transition to k occurs, given the previous transition was $i \to J$ is:

$$\tilde{\psi}_{iJk}(s) = \frac{\boldsymbol{p}_{iJ}^T}{\sum_{j\in J} p_{ij}}[\mathbb{I} - \tilde{\boldsymbol{\Psi}}_{JJ}(s)]^{-1}\tilde{\boldsymbol{\psi}}_{Jk}(s) \tag{2.6}$$

where

$$\tilde{\boldsymbol{\psi}}_{Jk}^T(s) = [\tilde{\psi}_{j_1 k}(s), \tilde{\psi}_{j_2 k}(s), \cdots, \tilde{\psi}_{j_{N_j} k}(s)] \tag{2.7}$$

and $\tilde{\boldsymbol{\Psi}}_{JJ}(s)$ is a matrix of the Laplace transforms of every joint probability distribution of waiting times and transitions within J:

$$\tilde{\boldsymbol{\Psi}}_{JJ}(s) = \begin{cases} \tilde{\psi}_{j_m j_n}(s) & m \neq n \\ 0 & m = n \end{cases} \tag{2.8}$$

We denote $\tilde{\psi}_{iJK}(s) \equiv \sum_{k\in K} \tilde{\psi}_{iJk}(s)$. Then, the Laplace transform of the conditional waiting time distribution is:

$$\tilde{\psi}_{IJK}(s) = \sum_{i\in I} \frac{\pi_i}{\pi_I} \frac{\tilde{\psi}_{iJK}(s)}{\tilde{\psi}_{iJK}(s \to 0)} \tag{2.9}$$

Finally, we apply an inverse Laplace transform to obtain the conditional probability density:

$$\psi_{IJK}(t) = \mathcal{L}^{-1}\{\psi_{IJK}(s)\} \tag{2.10}$$

We further impose mass conservation at each of the Markovian states according to Eq. 1.5, to make sure the solution represents a valid Markovian system.

2.1.2 Formalizing the optimization problem

Let $\mathcal{S}$ be the real underlying Markovian system and let $\mathcal{R}$ be a general underlying system with the same topology as $\mathcal{S}$, i.e., the same states and possible transitions as $\mathcal{S}$, but $\mathcal{R}$ can have arbitrary mass rates and steady-state probabilities. Given the set of all systems $\mathcal{R}$ with the same steady-state probabilities $\pi_I^{\mathcal{R}} = \pi_I^{\mathcal{S}}$, same first-order mass rates $n_{IJ}^{\mathcal{R}} = n_{IJ}^{\mathcal{S}}$, same second-order mass rates $n_{IJK}^{\mathcal{R}} = n_{IJK}^{\mathcal{S}}$, and the same conditional waiting time distributions $\psi_{IJK}^{\mathcal{R}}(t) = \psi_{IJK}^{\mathcal{S}}(t)$, as the system $\mathcal{S}$, the following inequality holds for the EPR of $\mathcal{S}$ and $\mathcal{R}$, $\sigma(\mathcal{S})$ and $\sigma(\mathcal{R})$, respectively:

$$\begin{aligned}\sigma_{\mathrm{tot}}(\mathcal{S}) \geq \min_{\mathcal{R}}\{\sigma_{\mathrm{tot}}(\mathcal{R}) | \forall_{I,J,K} : \pi_I^{\mathcal{R}} = \pi_I^{\mathcal{S}}, n_{IJ}^{\mathcal{R}} = n_{IJ}^{\mathcal{S}}, \\ n_{IJK}^{\mathcal{R}} = n_{IJK}^{\mathcal{S}}, \\ \psi_{IJK}^{\mathcal{R}}(t) = \psi_{IJK}^{\mathcal{S}}(t)\} \equiv \sigma_{\mathrm{opt}}^{(\infty)}\end{aligned} \tag{2.11}$$

where $\sigma_{\mathrm{opt}}^{(\infty)}$ is the minimal EPR value of all the possible underlying systems $\mathcal{R}$. The inequality holds since the real system $\mathcal{S}$ belongs to the set of systems over which we minimize. The only variables of the optimization problem are n_{ij} and π_i, from which one can fully describe any of the possible underlying Markovian systems $\mathcal{R}$. All the constraints, π_I, n_{IJ}, n_{IJK}, and $\psi_{IJK}(t)$, as well as the EPR objective function, depend on these variables. Note that these variables are bounded by $0 \leq \pi_i \leq \pi_I$ and $0 \leq n_{ij} \leq n_{IJ}$.

In contrast to the constraints on the steady-state probabilities and the first- and second-order mass rate values, the constraint on the waiting-time distributions requires an equality of continuous functions $\psi_{IJK}(t)$, which one cannot fully reconstruct from trajectory data of finite duration. Moreover, solving the optimization problem using a constraint on a function with non-trivial dependency on the optimization problem variables is extremely challenging. Thus, we modify the optimization, and instead, use the moments of the waiting time distributions:

$$\begin{aligned}\sigma_{\mathrm{opt}}^{(n)}(\mathcal{S}) \equiv \min_{\mathcal{R}}\{\sigma_{\mathrm{tot}}(\mathcal{R}) | \forall_{I,J,K} : \pi_I^{\mathcal{R}} = \pi_I^{\mathcal{S}}, n_{IJ}^{\mathcal{R}} = n_{IJ}^{\mathcal{S}}, \\ n_{IJK}^{\mathcal{R}} = n_{IJK}^{\mathcal{S}}, \\ \forall_{k\in\{1,2,\ldots,n\}} : \langle t_{IJK}^k \rangle^{\mathcal{R}} = \langle t_{IJK}^k \rangle^{\mathcal{S}}\}\end{aligned} \tag{2.12}$$

where $\langle t_{IJK}^k \rangle$ is the k-th moment of the conditional waiting time distribution $\psi_{IJK}(t)$. Using an increasing number of moments, we can write the hierarchical bounds:

$$\forall_{n\in\mathbb{N}} : \sigma_{\text{tot}}(\mathcal{S}) \geq \sigma_{\text{opt}}^{(\infty)}(\mathcal{S}) \geq \sigma_{\text{opt}}^{(n)}(\mathcal{S}) \geq \cdots \geq \sigma_{\text{opt}}^{(1)}(\mathcal{S}) \tag{2.13}$$

We can easily get the analytical expressions for the moments $\langle t_{IJK}^k \rangle$ from the Laplace transform (see Appendix B):

$$\langle t_{IJK}^k \rangle = (-1)^k \frac{d^k \tilde{\psi}_{IJK}(s)}{ds^k}|_{s\to 0} \tag{2.14}$$

Now, for each moment, we have an expression that depends on the optimization problem variables in a simpler way, which in turn, simplifies the calculations. After calculating the values of the observables for the optimization problem, we solve it using a global search non-linear optimization algorithm [75].

3

Results

3.1 Examples

We apply our proposed estimator to several model systems and compare its performance to the previous bounds on the total EPR.

3.1.1 4-state system

We consider a fully-connected network of 4 states, with two Markovian observed states $\{1, 2\}$ and two hidden states $\{3, 4\}$, which are coarse-grained to state H (Fig. 3.1(a)), resulting in second-order semi-Markov dynamics [64]. The observed statistics of interest are the steady state probabilities π_1, π_2 and π_H, the first-order mass rates n_{1H}, n_{H1}, n_{2H}, and n_{H2}, the second-order mass rates n_{1H2} and n_{2H1} and the k-th moment of the conditional waiting time distributions $\langle t^k_{1H1}\rangle$, $\langle t^k_{1H2}\rangle$, $\langle t^k_{2H1}\rangle$ and $\langle t^k_{2H2}\rangle$. Notice we only used the second-order statistics through the coarse-grained state H, since states 1 and 2 are Markovian. Furthermore, we do not use n_{1H1} and n_{2H2} since they depend on the other mass rates: $n_{1H1} = n_{1H} - n_{1H2}$ and $n_{2H2} = n_{2H} - n_{2H1}$. The derivations of the analytical expressions of the second-order mass rates and the moments of the conditional waiting time moments, for this system, can be found in Appendix C.

We tune the transition rates over the observed link between states 1 and 2

according to $w_{12}(F) = w_{12}e^{-\beta FL}$ and $w_{21}(F) = w_{21}e^{\beta FL}$, where $\beta = T^{-1}$ is the inverse temperature (with $k_{\mathrm{B}} = 1$), and L is a characteristic length scale, to mimic external forcing. We compare the different EPR estimators on the system for several values for a driving force F over the observed link (Fig. 3.1(b)).

The passive partial EPR [49]:

$$\begin{aligned}\sigma_{\mathrm{pp}} &= (\pi_1 w_{12} - \pi_2 w_{21}) \log\left(\frac{\pi_1 w_{12}}{\pi_2 w_{21}}\right) \\ &= (n_{12} - n_{21}) \log\left(\frac{n_{12}}{n_{21}}\right)\end{aligned} \tag{3.1}$$

The KLD estimator is the sum of two contributions:

$$\begin{aligned}\sigma_{\mathrm{KLD}} &= \sigma_{\mathrm{aff}} + \sigma_{\mathrm{WTD}} \\ &= \frac{1}{\mathcal{T}} \sum_{I,J,K} p_{IJK} \log\left(\frac{p([IJ] \to [JK])}{p([KJ] \to [JI])}\right) \\ &+ \frac{1}{\mathcal{T}} \sum_{I,J,K} p_{IJK} D\left[\psi_{IJK}(t) || \psi_{KJI}(t)\right]\end{aligned} \tag{3.2}$$

where $p([IJ] \to [JK])$ is the probability to observe the transition $J \to K$ given the previous transition was $I \to J$, p_{IJK} is the probability to observe the second-order transition $I \to J \to K$, and $D[p||q]$ is the KLD between the probability distributions p and q. As was previously shown, the hierarchy between the EPR estimators is $\sigma_{\mathrm{KLD}} \geq \sigma_{\mathrm{aff}} \geq \sigma_{\mathrm{pp}}$ [49, 64].

The σ_2 estimator is also formulated as an optimization problem searching over a canonical form of the system with the same observed statistics, however, it only considers the first- and second-order mass rates [69]. Its place in the hierarchy between the EPR estimators varies for different systems. While σ_2 can be greater than σ_{KLD} in some cases [69], here, for the rate values we used, $\sigma_2 < \sigma_{\mathrm{KLD}}$. In fact, although the values of σ_2 and σ_{aff} appear to be similar (Fig. 3.1(b)), actually $\sigma_2 < \sigma_{\mathrm{aff}}$ for all of the values of F used.

At the stalling force, there is no current in the visible link, and we get $\sigma_{\mathrm{pp}} = \sigma_{\mathrm{aff}} = \sigma_2 = 0$, which is the trivial bound. In contrast, σ_{KLD} and our estimator $\sigma_{\mathrm{opt}}^{(1)}$ give a non-trivial bound. Moreover, $\sigma_{\mathrm{opt}}^{(1)}$ surpasses σ_{KLD} significantly and yields a tight bound. For this system, using higher moments in order to calculate $\sigma_{\mathrm{opt}}^{(2)}$ did not make any improvement compared to $\sigma_{\mathrm{opt}}^{(1)}$.

While the example in this section is of a system with 3 observed states, 2 of which are Markovian, our approach can be generalized to any system. For example, see Appendix E for a system with 4 observed states, 3 of which are Markovian, where the $\sigma^{(1)}_{\text{opt}}$ estimator still outperforms σ_{KLD} and σ_2.

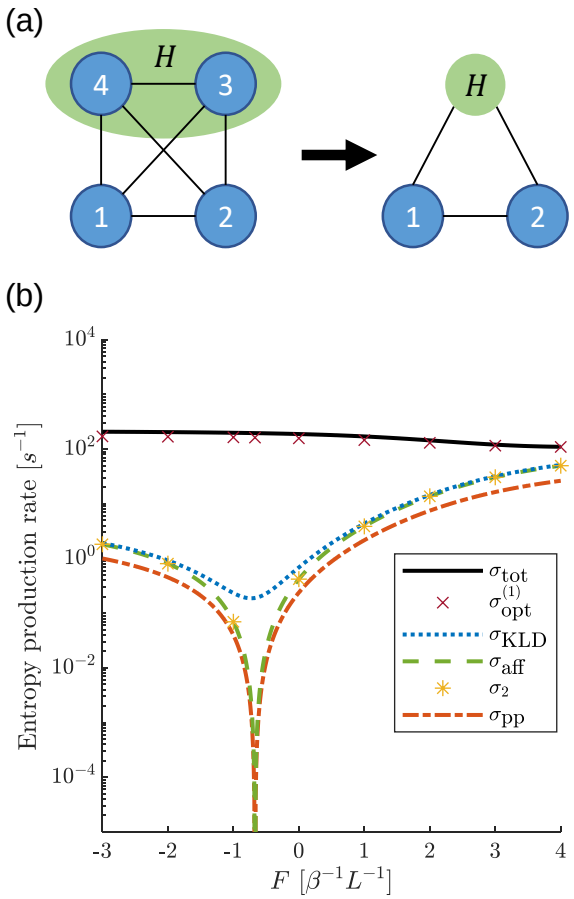

Figure 3.1: 4-state system. (a) Illustration of the full 4-state system topology, including the coarse-graining of states 3 and 4 to state H. (b) Total EPR $\sigma_{\rm tot}$ (solid black line), our bound $\sigma^{(1)}_{\rm opt}$ (brown cross), KLD estimator $\sigma_{\rm KLD}$ (dotted blue line), affinity estimator $\sigma_{\rm aff}$ (dashed green line), two-step estimator σ_2 (yellow Asterisk), and the passive partial entropy production $\sigma_{\rm pp}$ (dashed-dotted orange line). The rates we used are $w_{12} = 3\ s^{-1}$, $w_{13} = 0\ s^{-1}$, $w_{14} = 8\ s^{-1}$, $w_{21} = 2\ s^{-1}$, $w_{23} = 50\ s^{-1}$, $w_{24} = 0.2\ s^{-1}$, $w_{31} = 0\ s^{-1}$, $w_{32} = 2\ s^{-1}$, $w_{34} = 75\ s^{-1}$, $w_{41} = 1\ s^{-1}$, $w_{42} = 35\ s^{-1}$, $w_{43} = 0.7\ s^{-1}$.

3.1.2 Molecular motor

Here, we study a model of a molecular motor, illustrated in Fig. 3.2(a). The motor can physically move in space (upward or downward), $i \leftrightarrow i+1$, or change internal states (passive or active), $i \leftrightarrow i'$. An external source of chemical work $\Delta\mu$ drives the upward spatial jumps from the active state, and a mechanical force F acts against it and drives the downward transitions. We assume that an external observer cannot distinguish between the internal states of the motor, but rather can only record its physical position. The observed statistics are thus of a second-order Semi-Markov process [64].

Owing to the transnational symmetry in the model, we represent the molecule motor as a cyclic network of three coarse-grained states where each of them represents the physical location, lumping the active and passive internal states. We denote the steady-state probability of being in the passive and active states as π and π', respectively. Notice that the probability of being in each physical location in the 3-state cyclic system is the same, and that π and π' are the same for all of the physical locations, therefore, $\pi + \pi' = 1/3$.

We denote the upward and downward transitions from and to the passive state as u_1 and d_1, respectively, the upward and downward transitions from and to the active state as u_2 and d_2, respectively, and the transitions between the active and passive states at the same physical location as r (right) and l (left), respectively. The upward and downward coarse-grained transitions are labeled as U and D, respectively.

The observed statistics of interest are the first-order mass rates n_U, n_D, the second-order mass rates n_{UU}, n_{DD} and the k-th moment of the conditional waiting times $\langle t^k_{UU}\rangle$, $\langle t^k_{UD}\rangle$, $\langle t^k_{DU}\rangle$ and $\langle t^k_{DD}\rangle$. Note that we do not use n_{UD} and n_{DU}, since they depend on the other mass rates: $n_{UD} = n_U - n_{UU}$ and $n_{DU} = n_D - n_{DD}$. Owing to the symmetry of the cycle representation of the coarse-grained system, in which the steady-state probabilities are equally distributed, we only need the constraints on the upward and downward transitions. The derivations of the analytical expressions of the second-order mass rates and the moments of the conditional waiting time

distributions, for this system, can be found in Appendix D.

The chemical affinity μ, arising from ATP hydrolysis for example, only affects the transitions u_2 and d_2, whereas the external force F affects all of the spatial transitions u_1, d_1, u_2 and d_2. The transition rates then obey local detailed balance: $w_{d1}/w_{u1} = e^{\beta FL}$ and $w_{d2}/w_{u2} = e^{\beta(FL-\mu)}$, where L is the length of a single spatial jump [64].

We compare the different EPR estimators for the molecular motor system for several values of μ, and for each μ value, we tune the external forcing parameter F (Fig. 3.2(b)). Notice the passive partial EPR, $\sigma_{\rm pp}$, is not applicable for this system since all the original Markovian states are coarse-grained.

The hierarchy of the different EPR estimators for the molecular motor, for the rate values we used, is $\sigma_{\rm opt}^{(1)} \geq \sigma_{\rm KLD} \geq \sigma_{\rm aff} \geq \sigma_2$. At the stalling force for each value of μ, where there is no visible current, we find $\sigma_{\rm aff} = \sigma_2 = 0$, which is the trivial bound. In contrast, similar to the 4-state system, $\sigma_{\rm opt}^{(1)}$ surpasses $\sigma_{\rm KLD}$ significantly and yields a tight bound.

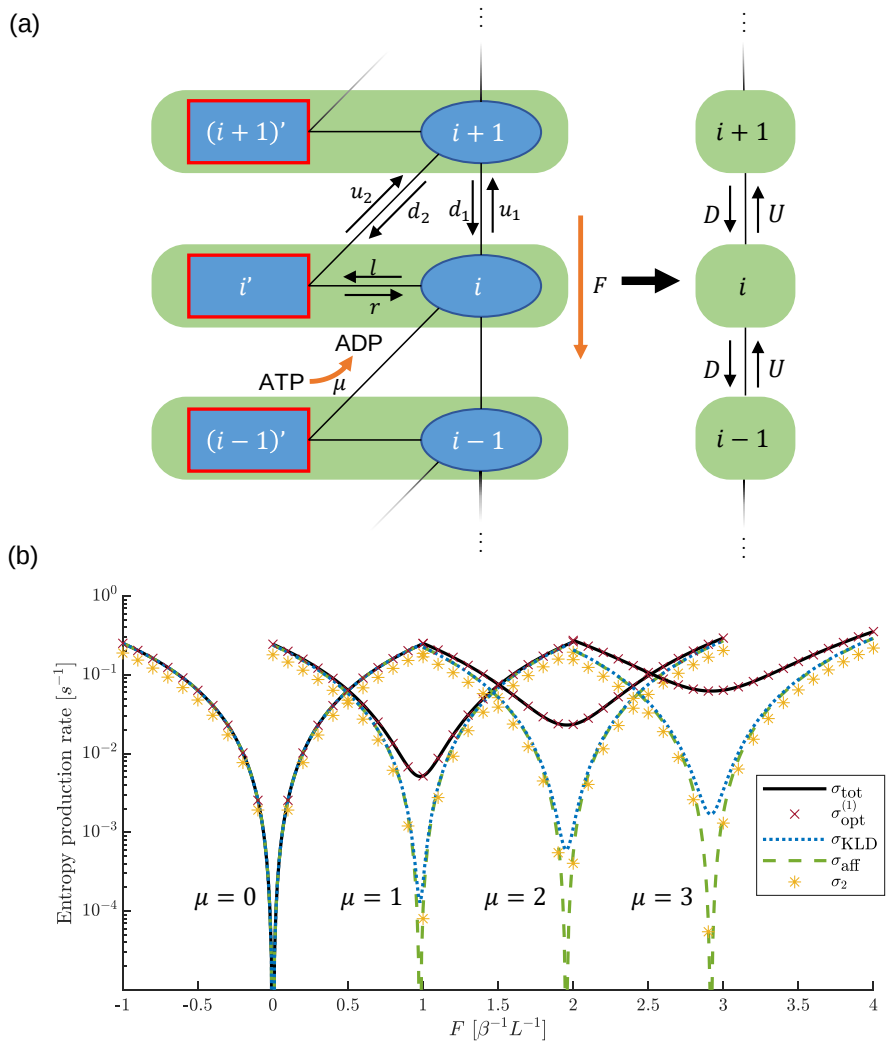

Figure 3.2: Molecular motor. (a) Illustration of the full molecular motor system including the coarse-graining of the active (red boxed square) and passive (ellipse) states. (b) Total EPR σ_{tot} (solid black line), our bound $\sigma^{(1)}_{\text{opt}}$ (brown cross), KLD estimator σ_{KLD} (dotted blue line), the affinity estimator σ_{aff} (dashed green line), and the two-step estimator σ_2 (yellow Asterisk). The rates we used are $w_r = w_l = w_{u2} = w_{d2} = 1\ s^{-1}$, $w_{u1} = w_{d1} = 0.01\ s^{-1}$.

3.2 Importance of data accuracy

One of the hyperparameters defining the optimization problem is the constraint tolerance, which indicates the acceptable numerical error of the solution. If ϵ is the absolute error of the trajectory statistics with respect to the true analytical ones, then the constraint tolerance must be equal to or greater than ϵ. Otherwise, when the constraint tolerance is smaller than the absolute error of the statistics, the optimization problem might not converge or give an overestimation in the worst-case scenario.

In Fig. 3.3, we plot the absolute (and relative) error of a few statistics values calculated from several trajectories as a function of the trajectory length N, for both systems discussed in the previous sections. Moreover, using the analytical values of the statistics for maximum accuracy, we plot the results of our estimator $\sigma^{(1)}_{\text{opt}}$ as a function of the constraint tolerance.

As expected, longer trajectory data result in a more accurate estimation of the observed statistics used for our optimization problem for both systems, as evident from the values of n_{1H}, n_{1H2} and $\langle t_{1H2} \rangle$ for the 4-state system (Fig. 3.3(a)), and from the values of n_U, n_{UU}, and $\langle t_{UU} \rangle$ for the molecular motor (Fig. 3.3(b)). For smaller errors, we can use a smaller constraint tolerance. The error bars in Fig. 3.3(a) and (b), which are the standard deviation of the values of the observables in different realizations of trajectories with the same size, can be used as a scale for the appropriate constraint tolerance.

For both systems, smaller constraint tolerance leads to a better estimator as the value of the lower bound on the EPR approaches the true analytical value (Fig. 3.3(c) and (d)), demonstrating the importance of an accurate estimation of the observables.

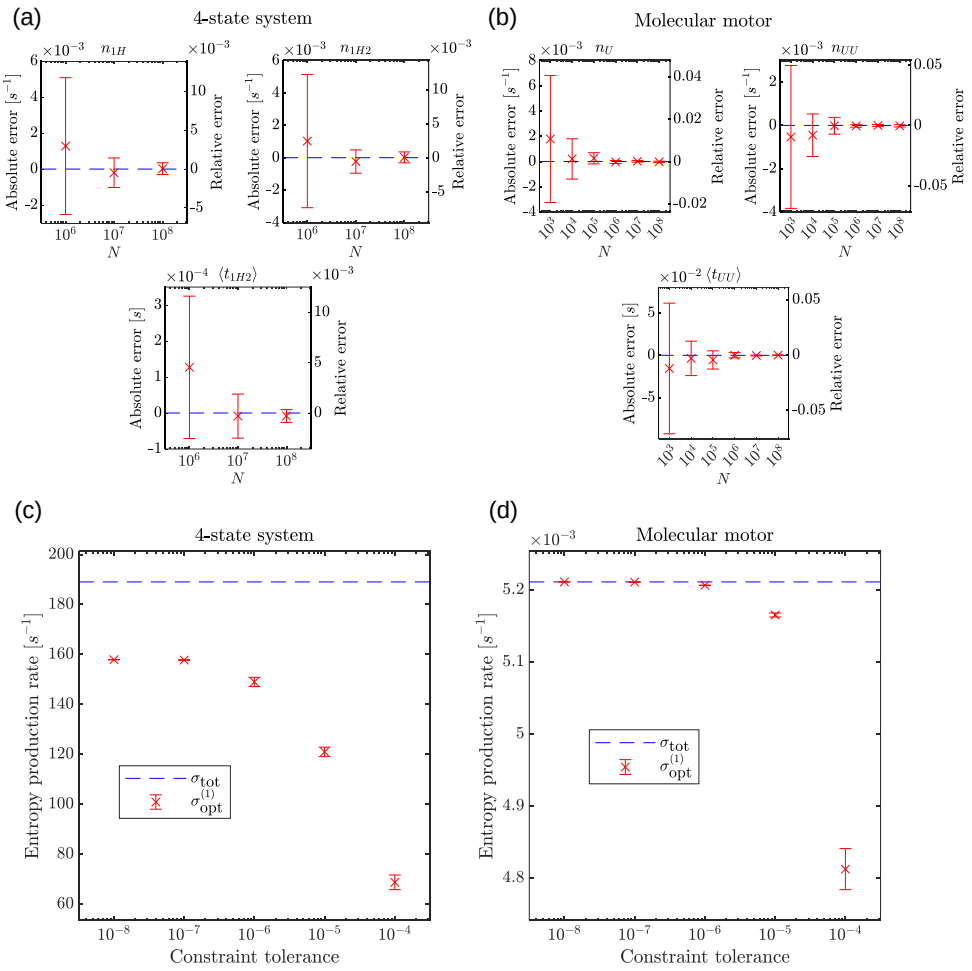

Figure 3.3: Importance of data accuracy. (a) The error of some statistics of the 4-state system for different values of the trajectory length N. The absolute and relative errors are on the left and right axes, respectively. (b) The error of some statistics of the molecular motor system for different values of the trajectory length N. The absolute and relative errors are on the left and right axes, respectively. (c) The error of $\sigma^{(1)}_{\rm opt}$ results for the 4-state system for different constraint tolerance values, using the analytical statistics values. (d) The error of $\sigma^{(1)}_{\rm opt}$ results for the molecular motor system for different constraint tolerance values, using the analytical statistics values. Error bars stand for the standard deviation of 10 different realizations.

3.3 Optimizing a simple model

Although our approach can be generalized to any number of hidden states, the analytical expressions for the observables become complicated, and the number of variables increases for a more complex coarse-grained topology. In turn, solving the optimization problem would require longer computation times. In order to test the performance of our estimator, we solved the optimization problem for a larger number of hidden states in a fully-connected network of 4, 5, and 6 states with only 2 Markovian observed states, assuming only 2 states are coarse-grained (Fig. 3.4(a)). Similarly, we tested the performance of our estimator for the case of the molecular motor with 2, 3, and 4 internal states at each physical position, assuming there are only 2. While generally, the estimator gives a more accurate result for the case of the 2 hidden state, which matches the assumption, it still provides a lower bound on the total EPR with comparable accuracy for a larger number of hidden states in the two systems (Fig. 3.4(b) and (c)). Moreover, our $\sigma^{(1)}_{\text{opt}}$ estimator can still outperform other estimators, σ_{KLD} and σ_2, as demonstrated for the case of a 5-state system with 2 Markovian observed states and one coarse-grained state of three internal states in Appendix F.

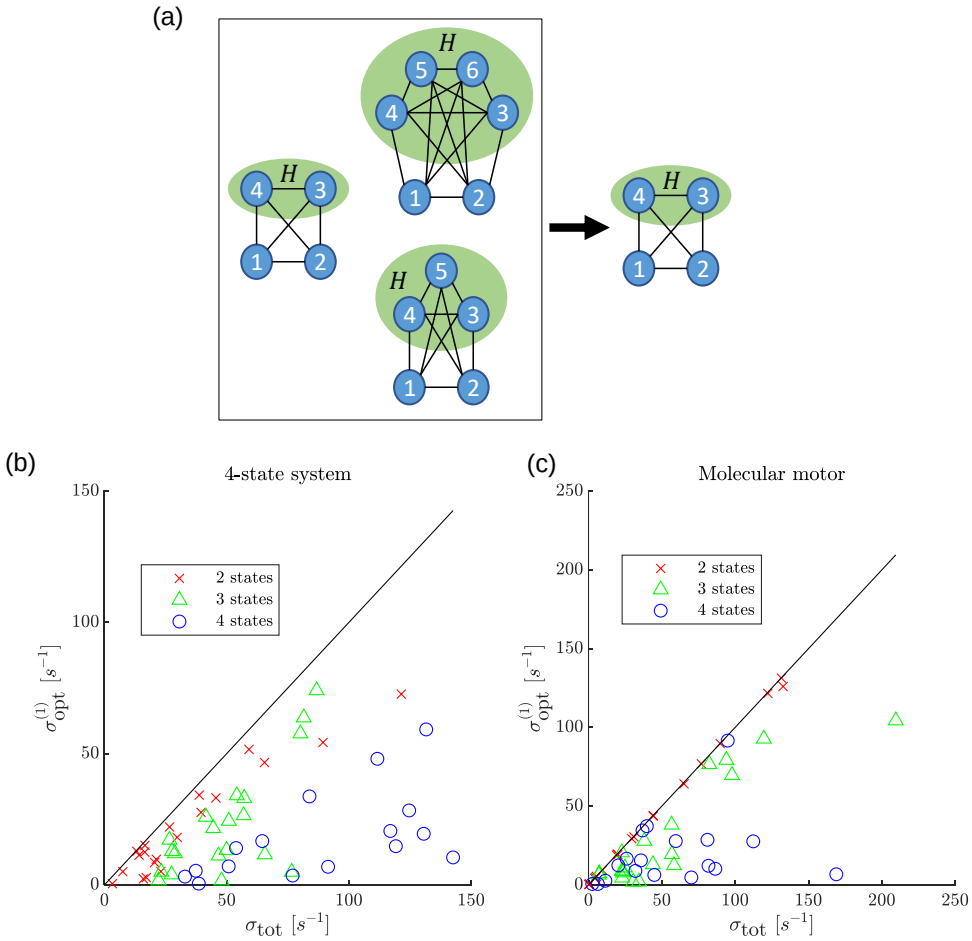

Figure 3.4: Optimizing using a simple model. (a) Illustration of solving the optimization problem for a simple model with 2 hidden states (right), whereas the real system has more hidden states (left). (b) The results of $\sigma^{(1)}_{\mathrm{opt}}$ assuming the simple 4-state model (2 hidden states), when the real system has 2 (red cross), 3 (green triangle) or 4 (blue circle) hidden states. (c) The results of $\sigma^{(1)}_{\mathrm{opt}}$ assuming the simple molecular motor model (2 hidden states), when the real system has 2 (red cross), 3 (green triangles) or 4 (blue circle) hidden states. For both systems, the results are presented for random generated transition rates (for each case) with statistics calculated from trajectories of length $N = 10^8$ using a constraint tolerance of 10^{-5}.

4

Conclusions

We present a new estimator for the entropy production rate, which gives a tight bound by formulating an optimization problem using both transitions and waiting times statistics. Such data is readily available in different experimental settings, for example, tracking a bead attached to a rotating bacterial flagellum [69, 76], or cortical granules embedded in the actomyosin cortex of an oocyte [77]. Our estimator can be applied to any system with a known topology, and it significantly surpasses previous estimators, as demonstrated for the two studied systems, the fully-connected hidden network, and the molecular motor. The variables for the optimization problem can be inferred from the observed statistics, where longer trajectories result in more accurate estimation and enable a smaller constraint tolerance value. Finally, for both systems, our approach can provide a lower bound on the total EPR for more complex systems, assuming a simpler underlying topology of the hidden states. Although we numerically showed that searching over all the systems with a simpler topology of the hidden part and the same observed statistics as the true system gave a lower bound on the total EPR for the two systems we studied, it remains an open problem to show this approach is universal. It would be interesting for future work to determine whether removing states from the hidden sub-network can only decrease the entropy production, given the observed statistics are conserved.

In summary, our approach is based on an optimization problem formulated using the observed statistics of a partially accessible system, utilizing information on the

underlying topology, in order to provide a tight lower bound on the total EPR. The estimator can be used as a benchmark for comparing the performance of other estimators that rely on coarse-grained or partial information about the system.

Appendices

Appendix A

Second-order mass rates

In order to find the second-order mass rates for two consecutive transitions between coarse-grained states, n_{IJK}, we need to take into account every possible original state $i \in I$, every possible path within the coarse-grained state J, and every possible transition from a state in J to every possible final state $k \in K$. Let us start by considering a specific initial Markovian state $i \in I$ and a specific final Markovian state $k \in K$ and calculate the mass rate n_{iJk}:

$$\begin{aligned} n_{iJk} &= \sum_{N=0}^{\infty} \sum_{j_0,\ldots,j_N \in J} n_{ij_0} p_{j_0 j_1} p_{j_1 j_2} \cdots p_{j_{N-1} j_N} p_{j_N k} \\ &= \sum_{N=0}^{\infty} \sum_{j',j'' \in J} n_{ij'} \left[\boldsymbol{P}_{JJ}^{N}\right]_{j'j''} p_{j''k} \\ &= \sum_{j',j'' \in J} n_{ij'} \left(\sum_{N=0}^{\infty} \left[\boldsymbol{P}_{JJ}^{N}\right]_{j'j''} \right) p_{j''k} \\ &= \sum_{j',j'' \in J} n_{ij'} \left[\mathbb{I} - \boldsymbol{P}_{JJ}\right]^{-1}_{j'j''} p_{j''k} \\ &= \boldsymbol{n}_{iJ}^{T} \left[\mathbb{I} - \boldsymbol{P}_{JJ}\right]^{-1} \boldsymbol{p}_{Jk} \end{aligned} \tag{A.1}$$

The two summations are for all the possible lengths N of trajectories within J, and all the optional paths with the given length $\{j_0, j_1, \cdots, j_N\}$ in J. From mass conservation, we can now obtain the expression for n_{IJK} by summing over all the optional original $i \in I$ and final $k \in K$ states:

$$n_{IJK} = \sum_{i \in I} \sum_{k \in K} n_{iJk} \tag{A.2}$$

Appendix B

Conditional waiting time moments

The waiting time at each Markovian state i is an exponentially distributed random variable $\psi_i(t)$ with mean waiting time $\tau_i = \lambda_i^{-1}$:

$$\psi_i(t) = \lambda_i e^{-\lambda_i t} \tag{B.1}$$

For the calculations, we used the joint distribution of the waiting time and the transition $i \to j$:

$$\psi_{ij}(t) = w_{ij} e^{-\lambda_i t} \tag{B.2}$$

Notice that $\psi_{ij}(t)$ is not normalized to 1 as $\int_0^\infty \psi_{ij}(t)dt = p_{ij}$.

The probability to observe a trajectory $\gamma_N : i_0 \to i_1 \to \cdots \to i_N$ with a total duration of T is:

$$\begin{aligned} &p(\gamma_N, T) = \\ &= \int_{\sum_{i=0}^{N-1} t_i = T} \psi_{i_0 i_1}(t_0)\psi_{i_1 i_2}(t_1)\cdots\psi_{i_{N-1} i_N}(t_{N-1}) \\ &\qquad dt_0 dt_1 \cdots dt_{N-1} \end{aligned} \tag{B.3}$$

Since this is a convolution, we can perform a Laplace transform to get a simpler formula of multiplications of Laplace transforms of Markovian joint distributions of waiting times and transitions:

$$\tilde{p}(\gamma_N, s) = \tilde{\psi}_{i_0 i_1}(s)\tilde{\psi}_{i_1 i_2}(s)\cdots\tilde{\psi}_{i_{N-1} i_N}(s) \tag{B.4}$$

where

$$\begin{aligned}\tilde{\psi}_{ij}(s) &= \int_0^\infty \psi_{ij}(t)e^{-st}dt = \int_0^\infty w_{ij}e^{-\lambda_i t}e^{-st}dt \\ &= w_{ij}\int_0^\infty e^{-(s+\lambda_i)t}dt = w_{ij}\left[-\frac{e^{-(s+\lambda_i)t}}{s+\lambda_i}\right]_0^\infty \\ &= \frac{w_{ij}}{s+\lambda_i}\end{aligned} \tag{B.5}$$

In order to calculate the moments of the conditional waiting time distribution $\psi_{IJK}(t)$ for the coarse-grained state J conditioned on an initial state in I and a final state in K, our strategy is to calculate its Laplace transform $\tilde{\psi}_{IJK}(s)$. We start by calculating $\tilde{\psi}_{iJk}(s)$ which is the Laplace transform of the waiting distribution in coarse-grained state J, before jumping to a specific Markovian state $k \in K$, given it came from a specific Markovian state $i \in I$. Since we want the waiting time in J, we sum over all of the paths with any length N inside J with a final transition to $k \in K$, $j_0 \to j_1 \to \cdots \to j_N \to k$, weighed by the probability to jump from $i \in I$ to the first state $j_0 \in J$:

$$\begin{aligned}&\tilde{\psi}_{iJk}(s) = \\ &= \sum_{N=0}^{\infty}\sum_{j_0,\ldots,j_N\in J}\frac{p_{ij_0}}{\sum_{j\in J}p_{ij}}\tilde{p}(j_0\to j_1\to\cdots\to j_N\to k,s) \\ &= \sum_{N=0}^{\infty}\sum_{j_0,\ldots,j_N\in J}\frac{p_{ij_0}}{\sum_{j\in J}p_{ij}}\tilde{\psi}_{j_0j_1}(s)\cdots\tilde{\psi}_{j_{N-1}j_N}(s)\tilde{\psi}_{j_Nk}(s) \\ &= \sum_{N=0}^{\infty}\sum_{j',j''\in J}\frac{p_{ij'}}{\sum_{j\in J}p_{ij}}\left[\tilde{\mathbf{\Psi}}_{JJ}(s)^N\right]_{j',j''}\tilde{\psi}_{j''k}(s) \\ &= \sum_{j',j''\in J}\frac{p_{ij'}}{\sum_{j\in J}p_{ij}}\sum_{N=0}^{\infty}\left[\tilde{\mathbf{\Psi}}_{JJ}(s)^N\right]_{j',j''}\tilde{\psi}_{j''k}(s) \\ &= \sum_{j',j''\in J}\frac{p_{ij'}}{\sum_{j\in J}p_{ij}}\left[\mathbb{I}-\tilde{\mathbf{\Psi}}_{JJ}(s)\right]^{-1}_{j',j''}\tilde{\psi}_{j''k}(s) \\ &= \frac{\boldsymbol{p}_{iJ}^T}{\sum_{j\in J}p_{ij}}\left[\mathbb{I}-\tilde{\mathbf{\Psi}}_{JJ}(s)\right]^{-1}\tilde{\boldsymbol{\psi}}_{Jk}(s)\end{aligned} \tag{B.6}$$

where $\tilde{\mathbf{\Psi}}_{JJ}(s)$ is a matrix of size $N_J \times N_J$, and N_J is the number of Markovian states

inside J:

$$\left[\tilde{\mathbf{\Psi}}_{JJ}(s)\right]_{j_1,j_2} = \begin{cases} \tilde{\Psi}_{j_1 j_2}(s) & j_1 \neq j_2 \\ 0 & j_1 = j_2 \end{cases} \tag{B.7}$$

As mentioned in the main text we denote $\tilde{\psi}_{iJK}(s) \equiv \sum_{k\in K} \tilde{\psi}_{iJk}(s)$. Notice that $\tilde{\psi}_{iJK}(s)$ is not normalized to 1 and it needs to be divided by $\tilde{\psi}_{iJK}(s \to 0)$, which is exactly the probability to jump from J to K, given the transition to J was from i.

$$\tilde{\psi}_{iJK}^{Normalized}(s) = \frac{\tilde{\psi}_{iJK}(s)}{\tilde{\psi}_{iJK}(s \to 0)} \tag{B.8}$$

This results from the fact that we used $\psi_{ij}(t)$, which is normalized to p_{ij}.

In order to get $\tilde{\psi}_{IJK}(s)$, we sum $\tilde{\psi}_{iJK}^{Normalized}(s)$ over all of the Markovian states $i \in I$, weighed by the corresponding probability π_i/π_I of being in state i, given the system is in the coarse-grained state I:

$$\tilde{\psi}_{IJK}(s) = \sum_{i\in I} \frac{\pi_i}{\pi_I} \tilde{\psi}_{iJK}^{Normalized}(s) \tag{B.9}$$

For a general probability density function $f(t) : [0,\infty] \to [0,1]$ the Laplace transform is:

$$\tilde{f}(s) = \int_0^\infty f(t) e^{-st} dt \tag{B.10}$$

and its k-th derivative by s is:

$$\frac{d^k \tilde{f}(s)}{ds^k} = (-1)^k \int_0^\infty t^k f(t) e^{-st} dt \tag{B.11}$$

Taking the limit $s \to 0$:

$$\begin{aligned} \frac{d^k \tilde{f}(s)}{ds^k}|_{s\to 0} &= (-1)^k \int_0^\infty t^k f(t) dt \\ &= (-1)^k \langle t^k \rangle \end{aligned} \tag{B.12}$$

we find the k-th moment of the probability density function $f(t)$:

$$\langle t^k \rangle = (-1)^k \frac{d^k \tilde{f}(s)}{ds^k}|_{s\to 0} \tag{B.13}$$

Therefore, the k-th moment $\langle t_{IJK}^k \rangle$ of the conditional waiting time distribution $\psi_{IJK}(t)$ is:

$$\langle t_{IJK}^k \rangle = (-1)^k \frac{d^k \tilde{\psi}_{IJK}(s)}{ds^k}|_{s\to 0} \tag{B.14}$$

Appendix C

Analytical expressions for the 4-state system

The variables to consider for this system are the mass rates n_{ij} and the steady-state probabilities π_i for $i, j \in \{1, 2, 3, 4\}$, meaning a total of 16 variables. Note that π_1, π_2, n_{12} and n_{21} are fully observed. Therefore, we are left with 12 variables. With the following linear constraints, we can immediately reduce the problem to 6 variables.

C.1 Linear constraints

We impose probability conservation, mass rate conservation in the hidden Markovian states, and mass rate conservation between an observed Markovian state and the hidden coarse-grained state.

C.1.1 Probabilities

From the conservation of the steady-state probability of the Markovian states within the coarse-grained hidden state:

$$\pi_H = \pi_3 + \pi_4 \tag{C.1}$$

C.1.2 Mass conservation at any Markovian state

We write the mass conservation for one of the hidden states (3 or 4), which for this system, is enough to guarantee the mass conservation for the other hidden state:

$$n_{13} + n_{23} + n_{43} = n_{31} + n_{32} + n_{34} \tag{C.2}$$

C.1.3 First-order mass rates

Here, we require the mass rate conservation of transitions in and out of the hidden state, providing 4 constraint equations:

$$\begin{aligned} \forall_{i\in\{1,2\}} &: n_{iH} = n_{i3} + n_{i4} \\ \forall_{i\in\{1,2\}} &: n_{Hi} = n_{3i} + n_{4i} \end{aligned} \tag{C.3}$$

C.2 Non-linear constraints

The second-order mass rates and the conditional waiting times moments can be expressed only as a non-linear function of the optimization problem variables. Here, we show the full derivations of these relations.

C.2.1 Second-order mass rates

For this system, as mentioned in the text, we are interested in n_{1H2} and n_{2H1}, where the first and the last states are the observed Markovian states. From equation Eq. A.1:

$$n_{iHj} = \boldsymbol{n}_{iH}^T \left[\mathbb{I} - \boldsymbol{P}_{HH}\right]^{-1} \boldsymbol{p}_{Hj} \tag{C.4}$$

Where

$$\boldsymbol{P}_{HH} = \begin{bmatrix} 0 & p_{34} \\ p_{43} & 0 \end{bmatrix} \tag{C.5}$$

and

$$\left[\mathbb{I} - \boldsymbol{P}_{HH}\right]^{-1} = \frac{1}{1 - p_{34}p_{43}} \begin{bmatrix} 1 & p_{34} \\ p_{43} & 1 \end{bmatrix} \tag{C.6}$$

Plugging into Eq. C.4, we have:

$$\begin{aligned} n_{iHj} &= \boldsymbol{n}_{iH}^T \left[\mathbb{I} - \boldsymbol{P}_{HH}\right]^{-1} \boldsymbol{p}_{Hj} \\ &= \begin{bmatrix} n_{i3} & n_{i4} \end{bmatrix} \left(\frac{1}{1 - p_{34}p_{43}} \begin{bmatrix} 1 & p_{34} \\ p_{43} & 1 \end{bmatrix} \right) \begin{bmatrix} p_{3j} \\ p_{4j} \end{bmatrix} \\ &= \frac{1}{1 - p_{34}p_{43}} \begin{bmatrix} n_{i3} & n_{i4} \end{bmatrix} \begin{bmatrix} p_{3j} + p_{34}p_{4j} \\ p_{4j} + p_{43}p_{3j} \end{bmatrix} \\ &= \frac{n_{i3}(p_{3j} + p_{34}p_{4j}) + n_{i4}(p_{4j} + p_{43}p_{3j})}{1 - p_{34}p_{43}} \end{aligned} \tag{C.7}$$

Remember we can express p_{ij} in terms of the mass rates (Eq. 1.3).

C.2.2 Conditional waiting time moments

We calculate the conditional waiting times moments $\langle t_{iHj}^k \rangle$ for $i, j \in \{1, 2\}$, in terms of the problem variables. Based on Eq. B.14, we need to calculate $\tilde{\psi}_{iHj}^{Normalized}(s)$.

From Eq. B.6:

$$\tilde{\psi}_{iHj}(s) = \frac{\boldsymbol{p}_{iH}^T}{\sum\limits_{h \in \{3,4\}} p_{ih}} \left[\mathbb{I} - \tilde{\boldsymbol{\Psi}}_{HH}(s)\right]^{-1} \tilde{\boldsymbol{\psi}}_{Hj}(s) \tag{C.8}$$

Now, we can calculate $\tilde{\boldsymbol{\psi}}_{Hj}(s)$ from Eq. 2.7 and Eq. B.5:

$$\tilde{\boldsymbol{\psi}}_{Hj}(s) = \begin{bmatrix} \tilde{\psi}_{3j}(s) \\ \tilde{\psi}_{4j}(s) \end{bmatrix} = \begin{bmatrix} \dfrac{w_{3j}}{s + \lambda_3} \\ \dfrac{w_{4j}}{s + \lambda_4} \end{bmatrix} \tag{C.9}$$

Given that (Eq. B.7 and Eq. B.5):

$$\begin{aligned} \tilde{\boldsymbol{\Psi}}_{HH}(s) &= \begin{bmatrix} 0 & \tilde{\psi}_{34}(s) \\ \tilde{\psi}_{43}(s) & 0 \end{bmatrix} \\ &= \begin{bmatrix} 0 & \dfrac{w_{34}}{s + \lambda_3} \\ \dfrac{w_{43}}{s + \lambda_4} & 0 \end{bmatrix} \end{aligned} \tag{C.10}$$

We can plug into Eq. C.8:

$$
\begin{aligned}
&\tilde{\psi}_{iHj}(s) = \\
&= \frac{\boldsymbol{p}_{iH}^T}{\sum_{h\in\{3,4\}} p_{ih}} \left[\mathbb{I} - \tilde{\boldsymbol{\Psi}}_{HH}(s)\right]^{-1} \tilde{\boldsymbol{\psi}}_{Hj}(s) \\
&= \frac{1}{p_{i3}+p_{i4}} \begin{bmatrix} p_{i3} & p_{i4} \end{bmatrix} \\
&\quad \left(\left(1 - \frac{w_{34}w_{43}}{(s+\lambda_3)(s+\lambda_4)}\right)^{-1} \begin{bmatrix} 1 & \frac{w_{34}}{s+\lambda_3} \\ \frac{w_{43}}{s+\lambda_4} & 1 \end{bmatrix} \right) \\
&\quad \begin{bmatrix} \frac{w_{3j}}{s+\lambda_3} \\ \frac{w_{4j}}{s+\lambda_4} \end{bmatrix} \\
&= \frac{1}{p_{i3}+p_{i4}} \left(1 - \frac{w_{34}w_{43}}{(s+\lambda_3)(s+\lambda_4)}\right)^{-1} \\
&\quad \begin{bmatrix} p_{i3} & p_{i4} \end{bmatrix} \begin{bmatrix} \frac{w_{3j}}{s+\lambda_3} + \frac{w_{34}}{s+\lambda_3}\frac{w_{4j}}{s+\lambda_4} \\ \frac{w_{4j}}{s+\lambda_4} + \frac{w_{43}}{s+\lambda_4}\frac{w_{3j}}{s+\lambda_3} \end{bmatrix} \\
&= \left(1 - \frac{w_{34}w_{43}}{(s+\lambda_3)(s+\lambda_4)}\right)^{-1} \\
&\quad \left[\frac{p_{i3}}{p_{i3}+p_{i4}} \left(\frac{w_{3j}}{s+\lambda_3} + \frac{w_{34}}{s+\lambda_3}\frac{w_{4j}}{s+\lambda_4} \right) \right. \\
&\quad \left. + \frac{p_{i4}}{p_{i3}+p_{i4}} \left(\frac{w_{4j}}{s+\lambda_4} + \frac{w_{43}}{s+\lambda_4}\frac{w_{3j}}{s+\lambda_3} \right) \right]
\end{aligned}
\tag{C.11}
$$

Since the states i and j are Markovian, we just need to normalize this expression in order to get the desired result:

$$
\begin{aligned}
&\tilde{\psi}_{iHj}(s \to 0) = \\
&= \left(1 - \frac{w_{34}w_{43}}{\lambda_3\lambda_4}\right)^{-1} \\
&\quad \left[\frac{p_{i3}}{p_{i3}+p_{i4}} \left(\frac{w_{3j}}{\lambda_3} + \frac{w_{34}}{\lambda_3}\frac{w_{4j}}{\lambda_4} \right) \right. \\
&\quad \left. + \frac{p_{i4}}{p_{i3}+p_{i4}} \left(\frac{w_{4j}}{\lambda_4} + \frac{w_{43}}{\lambda_4}\frac{w_{3j}}{\lambda_3} \right) \right] \\
&= \frac{p_{i3}\left(p_{3j} + p_{34}p_{4j}\right) + p_{i4}\left(p_{4j} + p_{43}p_{3j}\right)}{\left(p_{i3}+p_{i4}\right)\left(1 - p_{34}p_{43}\right)}
\end{aligned}
\tag{C.12}
$$

Therefore:

$$
\tilde{\psi}_{iHj}^{Normalized}(s) = \frac{\tilde{\psi}_{iHj}(s)}{\tilde{\psi}_{iHj}(s \to 0)} \tag{C.13}
$$

Finally, we get the moments from Eq. B.14.

In order to get the expressions of the derivatives, we used the package Sympy in Python.

Appendix D

Analytical expressions for the molecular motor system

The variables to consider for the molecular motor system are the mass rates n_{u1}, n_{u2}, n_{d1}, n_{d2}, n_l, n_r and the steady-state probabilities π and π', meaning a total of 8 variables. With the following linear constraints, we can immediately reduce the problem to 4 variables.

D.1 Linear constraints

As in the 4-state system, we impose probability conservation, mass rate conservation in the Markovian states, and mass rate conservation for the observed transitions U and D.

D.1.1 Probabilities

From the conservation of the steady-state probability of the Markovian states within the coarse-grained states:

$$\pi + \pi' = \frac{1}{3} \tag{D.1}$$

D.1.2 Mass conservation at any Markovian state

We write the mass conservation for one of the hidden states (active or passive), which for this system, is enough to guarantee the mass conservation for the other hidden state:

$$n_r + n_{u2} = n_l + n_{d2} \tag{D.2}$$

D.1.3 First-order mass rates

Here, we require the mass rate conservation of transitions in and out of the coarse-grained state, providing 2 constraint equations:

$$\begin{aligned} n_U &= n_{u1} + n_{u2} \\ n_D &= n_{d1} + n_{d2} \end{aligned} \tag{D.3}$$

D.2 Non-linear constraints

Since we have 2 hidden states as in the 4-state system, the results from Appendix C can be used here.

D.2.1 Second-order mass rates

We use the results for the 4-state system in Eq. C.7, together with Eq. A.2. For n_{UU}, we need to sum over all the mass that goes up from the passive or active state, and then up again only to the passive state:

$$\begin{aligned} n_{UU} &= \frac{n_{u1}(p_{u1} + p_l p_{u2})}{1 - p_l p_r} + \frac{n_{u2}(p_{u1} + p_l p_{u2})}{1 - p_l p_r} \\ &= \frac{(n_{u1} + n_{u2})(p_{u1} + p_l p_{u2})}{1 - p_l p_r} \end{aligned} \tag{D.4}$$

For n_{DD}, we need to sum over all the mass that goes down only from the passive

state, and then down again to the passive or active state:

$$\begin{aligned} n_{DD} &= \frac{n_{d1}p_{d1} + n_{d2}p_r p_{d1}}{1 - p_l p_r} + \frac{n_{d1}p_{d2} + n_{d2}p_r p_{d2}}{1 - p_l p_r} \\ &= \frac{(n_{d1} + n_{d2}p_r)(p_{d1} + p_{d2})}{1 - p_l p_r} \end{aligned} \tag{D.5}$$

D.2.2 Conditional waiting time moments

We account for all of the transitions through a coarse-grained state i, and specify in the following calculations the Markovian state before jumping to i, and the following Markovian state, after state i, where i' (i) denoted an active (passive) state. For example, $(i-1) \to (i+1)$ represent two consecutive transitions, $(i-1) \to i \to (i+1)$.

Note that a transition upward is only to a passive state, so the previous state (being passive or active) in the first transition does not affect the waiting time. Furthermore, a transition downward is only from a passive state.

From Eq. B.9:

$$\begin{aligned} \tilde{\psi}_{UU}(s) &= \frac{\pi}{\pi + \pi'} \frac{\tilde{\psi}_{(i-1)\to(i+1)}(s)}{\tilde{\psi}_{(i-1)\to(i+1)}(s \to 0)} \\ &\quad + \frac{\pi'}{\pi + \pi'} \frac{\tilde{\psi}_{(i-1)'\to(i+1)}(s)}{\tilde{\psi}_{(i-1)'\to(i+1)}(s \to 0)} \\ &= \frac{\tilde{\psi}_{(i-1)\to(i+1)}(s)}{\tilde{\psi}_{(i-1)\to(i+1)}(s \to 0)} \end{aligned} \tag{D.6a}$$

and similarly:

$$\begin{aligned} &\tilde{\psi}_{UD}(s) = \\ &= \frac{\pi}{\pi + \pi'} \frac{\left(\tilde{\psi}_{(i-1)\to(i-1)} + \tilde{\psi}_{(i-1)\to(i-1)'}\right)(s)}{\left(\tilde{\psi}_{(i-1)\to(i-1)} + \tilde{\psi}_{(i-1)\to(i-1)'}\right)(s \to 0)} \\ &+ \frac{\pi'}{\pi + \pi'} \frac{\left(\tilde{\psi}_{(i-1)'\to(i-1)} + \tilde{\psi}_{(i-1)'\to(i-1)'}\right)(s)}{\left(\tilde{\psi}_{(i-1)'\to(i-1)} + \tilde{\psi}_{(i-1)'\to(i-1)'}\right)(s \to 0)} \\ &= \frac{\left(\tilde{\psi}_{(i-1)\to(i-1)} + \tilde{\psi}_{(i-1)\to(i-1)'}\right)(s)}{\left(\tilde{\psi}_{(i-1)\to(i-1)} + \tilde{\psi}_{(i-1)\to(i-1)'}\right)(s \to 0)} \end{aligned} \tag{D.6b}$$

Moreover:

$$\tilde{\psi}_{DU}(s) = \frac{\tilde{\psi}_{(i+1)\to(i+1)}(s)}{\tilde{\psi}_{(i+1)\to(i+1)}(s \to 0)} \tag{D.6c}$$

and:

$$\tilde{\psi}_{DD}(s) = \frac{\left(\tilde{\psi}_{(i+1)\to(i-1)} + \tilde{\psi}_{(i+1)\to(i-1)'}\right)(s)}{\left(\tilde{\psi}_{(i+1)\to(i-1)} + \tilde{\psi}_{(i+1)\to(i-1)'}\right)(s \to 0)} \tag{D.6d}$$

Now we calculate all the terms in the numerators, using Eq. C.11 from the 4-state system results:

$$\begin{aligned}\tilde{\psi}_{(i-1)\to(i+1)}(s) = &\left(1 - \frac{w_l w_r}{(s+\lambda)(s+\lambda')}\right)^{-1} \\ &\left(\frac{w_{u1}}{s+\lambda} + \frac{w_l}{s+\lambda}\frac{w_{u2}}{s+\lambda'}\right)\end{aligned} \tag{D.7a}$$

$$\begin{aligned}&\left(\tilde{\psi}_{(i-1)\to(i-1)} + \tilde{\psi}_{(i-1)\to(i-1)'}\right)(s) = \\ &= \left(1 - \frac{w_l w_r}{(s+\lambda)(s+\lambda')}\right)^{-1}\left(\frac{w_{d1}}{s+\lambda} + \frac{w_{d2}}{s+\lambda}\right) \\ &= \left(1 - \frac{w_l w_r}{(s+\lambda)(s+\lambda')}\right)^{-1}\frac{w_{d1}+w_{d2}}{s+\lambda}\end{aligned} \tag{D.7b}$$

$$\begin{aligned}&\tilde{\psi}_{(i+1)\to(i+1)}(s) = \\ &= \left(1 - \frac{w_l w_r}{(s+\lambda)(s+\lambda')}\right)^{-1} \\ &\left[\frac{p_{d1}}{p_{d1}+p_{d2}}\frac{w_{u1}}{s+\lambda} + \frac{p_{d2}}{p_{d1}+p_{d2}}\frac{w_r}{s+\lambda'}\frac{w_{u1}}{s+\lambda}\right] \\ &= \left(1 - \frac{w_l w_r}{(s+\lambda)(s+\lambda')}\right)^{-1} \\ &\frac{1}{p_{d1}+p_{d2}}\frac{w_{u1}}{s+\lambda}\left[p_{d1} + \frac{p_{d2}w_r}{s+\lambda'}\right]\end{aligned} \tag{D.7c}$$

$$
\begin{aligned}
&\left(\tilde{\psi}_{(i+1)\to(i-1)} + \tilde{\psi}_{(i+1)\to(i-1)'}\right)(s) = \\
&= \left(1 - \frac{w_l w_r}{(s+\lambda)(s+\lambda')}\right)^{-1} \\
&\left[\frac{p_{d1}}{p_{d1}+p_{d2}}\frac{w_{d1}}{s+\lambda} + \frac{p_{d2}}{p_{d1}+p_{d2}}\frac{w_r}{s+\lambda'}\frac{w_{d1}}{s+\lambda}\right. \\
&\left.+\frac{p_{d1}}{p_{d1}+p_{d2}}\frac{w_{d2}}{s+\lambda} + \frac{p_{d2}}{p_{d1}+p_{d2}}\frac{w_r}{s+\lambda'}\frac{w_{d2}}{s+\lambda}\right] \\
&= \left(1 - \frac{w_l w_r}{(s+\lambda)(s+\lambda')}\right)^{-1} \\
&\left[\frac{p_{d1}}{p_{d1}+p_{d2}}\frac{w_{d1}+w_{d2}}{s+\lambda} + \frac{p_{d2}}{p_{d1}+p_{d2}}\frac{w_r}{s+\lambda'}\frac{w_{d1}+w_{d2}}{s+\lambda}\right] \\
&= \left(1 - \frac{w_l w_r}{(s+\lambda)(s+\lambda')}\right)^{-1} \\
&\frac{1}{p_{d1}+p_{d2}}\frac{w_{d1}+w_{d2}}{s+\lambda}\left[p_{d1} + \frac{p_{d2}w_r}{s+\lambda'}\right]
\end{aligned}
\tag{D.7d}
$$

All of the denominators from Eq. D.6 can be calculated by setting $s \to 0$ in Eq. D.7. Finally, we get the moments from equation Eq. B.14.

In order to get the expressions of the derivatives, we used the package Sympy in Python.

Appendix E

Larger systems

We apply our method to a system with 5 states, 3 of which are Markovian, and the other 2 are coarse-grained to a single state H (Fig. E.1(a)), for different values of an external force F used to tune the transition rates over the observed link $1-2$ according to $w_{12}(F) = w_{12}e^{-\beta FL}$ and $w_{21}(F) = w_{21}e^{\beta FL}$. Comparing the results of our method to other bounds (Fig. E.1(b)), $\sigma^{(1)}_{\text{opt}}$ outperforms σ_{KLD} and σ_2, and trivially σ_{aff}.

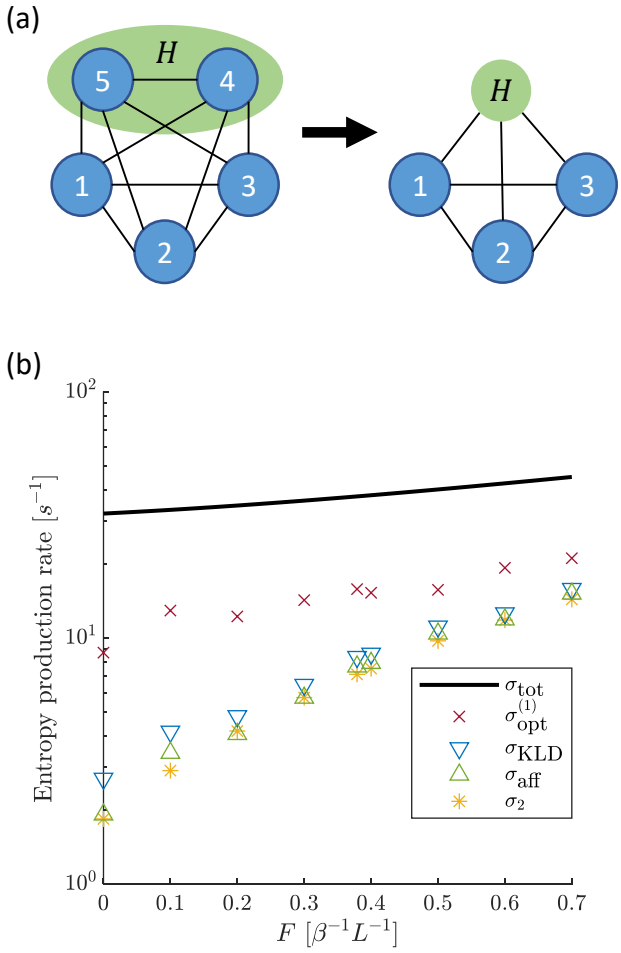

Figure E.1: 5-state system with four observed states. (a) Illustration of the full system topology, including the coarse-graining of states 4 and 5 to state H. (b) Total EPR σ_{tot} (black line), our bound $\sigma^{(1)}_{\mathrm{opt}}$ (red cross), KLD estimator σ_{KLD} (blue downward-pointing triangle), affinity estimator σ_{aff} (green upward-pointing triangle) and two-step estimator σ_2 (yellow Asterisk). The rates used are $w_{12} = 11\ s^{-1}$, $w_{13} = 0\ s^{-1}$, $w_{14} = 71\ s^{-1}$, $w_{15} = 81\ s^{-1}$, $w_{21} = 31\ s^{-1}$, $w_{23} = 0\ s^{-1}$, $w_{24} = 12\ s^{-1}$, $w_{21} = 96\ s^{-1}$, $w_{31} = 0\ s^{-1}$, $w_{32} = 0\ s^{-1}$, $w_{34} = 92\ s^{-1}$, $w_{35} = 12\ s^{-1}$, $w_{41} = 69\ s^{-1}$, $w_{42} = 15\ s^{-1}$, $w_{43} = 14\ s^{-1}$, $w_{45} = 91\ s^{-1}$, $w_{51} = 100\ s^{-1}$, $w_{52} = 71\ s^{-1}$, $w_{53} = 29\ s^{-1}$, $w_{54} = 30\ s^{-1}$.

Appendix F

Comparing estimators when optimizing for a simple model

We apply our method to a system with 5 states, 2 of which are Markovian, and the other 3 are coarse-grained to a single state H. In order to solve for a case where one does not have information about the underlying topology, we assume the simplest topology, with only 2 internal states (Fig. F.1a), and write the optimization problem accordingly. Using our approach, not only do we get a lower bound on the total EPR, but also our estimator $\sigma^{(1)}_{\text{opt}}$ outperforms the other estimators.

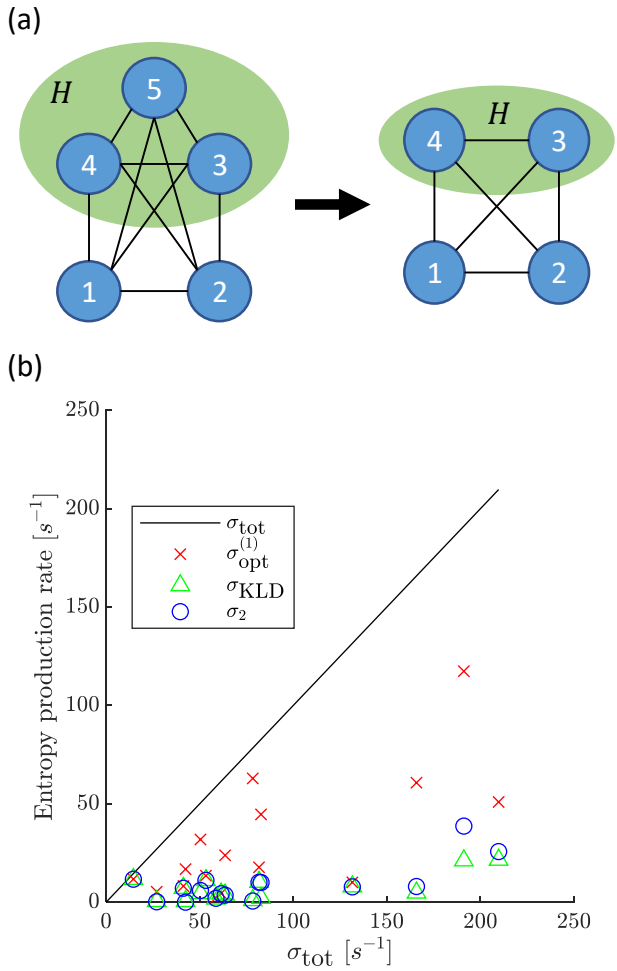

Figure F.1: Comparison to other bounds when assuming a simple topology. (a) Illustration of the full 5-state system topology, including the coarse-graining of states 3, 4, and 5 to state H (left) and the full-system topology we assume (right). (b) Total EPR σ_{tot} (solid black line), our bound $\sigma_{\mathrm{opt}}^{(1)}$ (red cross), KLD estimator σ_{KLD} (green upward-pointing triangle) and two-step estimator σ_2 (blue circle). The results are presented for randomly generated transition rates with statistics calculated from trajectories of length $N = 10^8$. Values of the estimators with the same σ_{tot} correspond to the same system, showing that $\sigma_{\mathrm{opt}}^{(1)}$ outperforms both σ_{KLD} and σ_2.

Bibliography

[1]E. Nitzan, A. Ghosal, and G. Bisker, "Universal bounds on entropy production inferred from observed statistics", arXiv preprint arXiv:2212.01783 (2022).

[2]C. J. Bustamante, Y. R. Chemla, S. Liu, and M. D. Wang, "Optical tweezers in single-molecule biophysics", Nature Reviews Methods Primers **1**, 1–29 (2021).

[3]C. D. Kinz-Thompson, K. K. Ray, and R. L. Gonzalez Jr, "Bayesian inference: the comprehensive approach to analyzing single-molecule experiments", Annual Review of Biophysics **50**, 191–208 (2021).

[4]C. Bustamante, L. Alexander, K. Maciuba, and C. M. Kaiser, "Single-molecule studies of protein folding with optical tweezers", Annual Review of Biochemistry **89**, 443 (2020).

[5]C. Bustamante, "Unfolding single rna molecules: bridging the gap between equilibrium and non-equilibrium statistical thermodynamics", Quarterly Reviews of Biophysics **38**, 291–301 (2005).

[6]U. Seifert, "Stochastic thermodynamics, fluctuation theorems and molecular machines", Reports on Progress in Physics **75**, 126001 (2012).

[7]C. Van den Broeck and M. Esposito, "Ensemble and trajectory thermodynamics: a brief introduction", Physica A: Statistical Mechanics and its Applications **418**, 6–16 (2015).

[8]R. Van Zon and E. Cohen, "Stationary and transient work-fluctuation theorems for a dragged brownian particle", Physical Review E **67**, 046102 (2003).

[9]F. Douarche, S. Joubaud, N. B. Garnier, A. Petrosyan, and S. Ciliberto, "Work fluctuation theorems for harmonic oscillators", Physical Review Letters **97**, 140603 (2006).

[10]S. Sabhapandit, "Heat and work fluctuations for a harmonic oscillator", Physical Review E **85**, 021108 (2012).

[11]P. Visco, "Work fluctuations for a brownian particle between two thermostats", Journal of Statistical Mechanics: Theory and Experiment **2006**, P06006 (2006).

[12]G. Wang, E. M. Sevick, E. Mittag, D. J. Searles, and D. J. Evans, "Experimental demonstration of violations of the second law of thermodynamics for small systems and short time scales", Physical Review Letters **89**, 050601 (2002).

[13]S. Ciliberto, A. Imparato, A. Naert, and M. Tanase, "Heat flux and entropy produced by thermal fluctuations", Physical Review Letters **110**, 180601 (2013).

[14]I. A. Martınez, É. Roldán, L. Dinis, D. Petrov, J. M. Parrondo, and R. A. Rica, "Brownian carnot engine", Nature Physics **12**, 67–70 (2016).

[15]C. Van den Broeck, N. Kumar, and K. Lindenberg, "Efficiency of isothermal molecular machines at maximum power", Physical Review Letters **108**, 210602 (2012).

[16]G. Verley, M. Esposito, T. Willaert, and C. Van den Broeck, "The unlikely carnot efficiency", Nature Communications **5**, 1–5 (2014).

[17]S. Mohanta, S. Saryal, and B. K. Agarwalla, "Universal bounds on cooling power and cooling efficiency for autonomous absorption refrigerators", Physical Review E **105**, 034127 (2022).

[18]S. Bo, M. Del Giudice, and A. Celani, "Thermodynamic limits to information harvesting by sensory systems", Journal of Statistical Mechanics: Theory and Experiment **2015**, P01014 (2015).

[19]N. P. Saadat, T. Nies, Y. Rousset, and O. Ebenhöh, "Thermodynamic limits and optimality of microbial growth", Entropy **22**, 277 (2020).

[20]J. Li, J. M. Horowitz, T. R. Gingrich, and N. Fakhri, "Quantifying dissipation using fluctuating currents", Nature Communications **10**, 1–9 (2019).

[21]É. Fodor, C. Nardini, M. E. Cates, J. Tailleur, P. Visco, and F. Van Wijland, "How far from equilibrium is active matter?", Physical Review Letters **117**, 038103 (2016).

[22]C. Maes and K. Netočnỳ, "Time-reversal and entropy", Journal of Statistical Physics **110**, 269–310 (2003).

[23]J. M. Parrondo, C. Van den Broeck, and R. Kawai, "Entropy production and the arrow of time", New Journal of Physics **11**, 073008 (2009).

[24]P. Pietzonka, A. C. Barato, and U. Seifert, "Universal bound on the efficiency of molecular motors", Journal of Statistical Mechanics: Theory and Experiment **2016**, 124004 (2016).

[25]N. Shiraishi, "Optimal thermodynamic uncertainty relation in markov jump processes", Journal of Statistical Physics **185**, 1–15 (2021).

[26]J. M. Horowitz and T. R. Gingrich, "Thermodynamic uncertainty relations constrain non-equilibrium fluctuations", Nature Physics **16**, 15–20 (2020).

[27]T. R. Gingrich, J. M. Horowitz, N. Perunov, and J. L. England, "Dissipation bounds all steady-state current fluctuations", Physical Review Letters **116**, 120601 (2016).

[28]A. C. Barato and U. Seifert, "Thermodynamic uncertainty relation for biomolecular processes", Physical Review Letters **114**, 158101 (2015).

[29]S. K. Manikandan, S. Ghosh, A. Kundu, B. Das, V. Agrawal, D. Mitra, A. Banerjee, and S. Krishnamurthy, "Quantitative analysis of non-equilibrium systems from short-time experimental data", Communications Physics **4**, 1–10 (2021).

[30]S. K. Manikandan, D. Gupta, and S. Krishnamurthy, "Inferring entropy production from short experiments", Physical Review Letters **124**, 120603 (2020).

[31]T. R. Gingrich and J. M. Horowitz, "Fundamental bounds on first passage time fluctuations for currents", Physical Review Letters **119**, 170601 (2017).

[32]A. Pal, S. Reuveni, and S. Rahav, "Thermodynamic uncertainty relation for first-passage times on markov chains", Physical Review Research **3**, L032034 (2021).

[33]I. Di Terlizzi and M. Baiesi, "Kinetic uncertainty relation", Journal of Physics A: Mathematical and Theoretical **52**, 02LT03 (2018).

[34]T. Van Vu, Y. Hasegawa, et al., "Unified thermodynamic–kinetic uncertainty relation", Journal of Physics A: Mathematical and Theoretical **55**, 405004 (2022).

[35]D. J. Skinner and J. Dunkel, "Estimating entropy production from waiting time distributions", Physical Review Letters **127**, 198101 (2021).

[36]A. Ghosal and G. Bisker, "Inferring entropy production rate from partially observed langevin dynamics under coarse-graining", Physical Chemistry Chemical Physics **24**, 24021–24031 (2022).

[37]U. Kapustin, A. Ghosal, and G. Bisker, "Utilizing time-series measurements for entropy production estimation in partially observed systems", arXiv preprint arXiv:2212.13487 (2022).

[38]S. Otsubo, S. Ito, A. Dechant, and T. Sagawa, "Estimating entropy production by machine learning of short-time fluctuating currents", Physical Review E **101**, 062106 (2020).

[39]D.-K. Kim, Y. Bae, S. Lee, and H. Jeong, "Learning entropy production via neural networks", Physical Review Letters **125**, 140604 (2020).

[40]Y. Bae, D.-K. Kim, and H. Jeong, "Inferring dissipation maps from videos using convolutional neural networks", Physical Review Research **4**, 033094 (2022).

[41]D.-K. Kim, S. Lee, and H. Jeong, "Estimating entropy production with odd-parity state variables via machine learning", Physical Review Research **4**, 023051 (2022).

[42]É. Roldán and J. M. Parrondo, "Estimating dissipation from single stationary trajectories", Physical Review Letters **105**, 150607 (2010).

[43]S. Otsubo, S. K. Manikandan, T. Sagawa, and S. Krishnamurthy, "Estimating time-dependent entropy production from non-equilibrium trajectories", Communications Physics **5**, 1–10 (2022).

[44]B. Lander, J. Mehl, V. Blickle, C. Bechinger, and U. Seifert, "Noninvasive measurement of dissipation in colloidal systems", Physical Review E **86**, 030401 (2012).

[45]P. Padmanabha, D. M. Busiello, A. Maritan, and D. Gupta, "Fluctuations of entropy production of a run-and-tumble particle", arXiv preprint arXiv:2207.12091 (2022).

[46]A. Dechant and S.-i. Sasa, "Entropic bounds on currents in langevin systems", Physical Review E **97**, 062101 (2018).

[47]R. Kawai, J. M. Parrondo, and C. Van den Broeck, "Dissipation: the phase-space perspective", Physical Review Letters **98**, 080602 (2007).

[48]G. Teza and A. L. Stella, "Exact coarse graining preserves entropy production out of equilibrium", Physical Review Letters **125**, 110601 (2020).

[49]G. Bisker, M. Polettini, T. R. Gingrich, and J. M. Horowitz, "Hierarchical bounds on entropy production inferred from partial information", Journal of Statistical Mechanics: Theory and Experiment **2017**, 093210 (2017).

[50]M. Esposito, "Stochastic thermodynamics under coarse graining", Physical Review E **85**, 041125 (2012).

[51]D. M. Busiello, J. Hidalgo, and A. Maritan, "Entropy production for coarse-grained dynamics", New Journal of Physics **21**, 073004 (2019).

[52]A. Ghosal and G. Bisker, "Entropy production rates for different notions of partial information", Journal of Physics D: Applied Physics (2023).

[53]P. J. Foster, J. Bae, B. Lemma, J. Zheng, W. Ireland, P. Chandrakar, R. Boros, Z. Dogic, D. J. Needleman, and J. J. Vlassak, "Dissipation and energy propagation across scales in an active cytoskeletal material", Proceedings of the National Academy of Sciences **120**, e2207662120 (2023).

[54]S. Ro, B. Guo, A. Shih, T. V. Phan, R. H. Austin, D. Levine, P. M. Chaikin, and S. Martiniani, "Model-free measurement of local entropy production and extractable work in active matter", Physical Review Letters **129**, 220601 (2022).

[55]D. Lucente, A. Baldassarri, A. Puglisi, A. Vulpiani, and M. Viale, "Inference of time irreversibility from incomplete information: linear systems and its pitfalls", Physical Review Research **4**, 043103 (2022).

[56]N. Shiraishi, S. Ito, K. Kawaguchi, and T. Sagawa, "Role of measurement-feedback separation in autonomous maxwell's demons", New Journal of Physics **17**, 045012 (2015).

[57]N. Shiraishi and T. Sagawa, "Fluctuation theorem for partially masked nonequilibrium dynamics", Physical Review E **91**, 012130 (2015).

[58]M. Polettini and M. Esposito, "Effective thermodynamics for a marginal observer", Physical Review Letters **119**, 240601 (2017).

[59]C. Maes, "The fluctuation theorem as a gibbs property", Journal of Statistical Physics **95**, 367–392 (1999).

[60]É. Roldán, J. Barral, P. Martin, J. M. Parrondo, and F. Jülicher, "Quantifying entropy production in active fluctuations of the hair-cell bundle from time irreversibility and uncertainty relations", New Journal of Physics **23**, 083013 (2021).

[61]J. Horowitz and C. Jarzynski, "Illustrative example of the relationship between dissipation and relative entropy", Physical Review E **79**, 021106 (2009).

[62]B. Gaveau, L. Granger, M. Moreau, and L. Schulman, "Dissipation, interaction, and relative entropy", Physical Review E **89**, 032107 (2014).

[63]B. Gaveau, L. Granger, M. Moreau, and L. S. Schulman, "Relative entropy, interaction energy and the nature of dissipation", Entropy **16**, 3173–3206 (2014).

[64]I. A. Martınez, G. Bisker, J. M. Horowitz, and J. M. Parrondo, "Inferring broken detailed balance in the absence of observable currents", Nature Communications **10**, 1–10 (2019).

[65]J. Van der Meer, B. Ertel, and U. Seifert, "Thermodynamic inference in partially accessible markov networks: a unifying perspective from transition-based waiting time distributions", Physical Review X **12**, 031025 (2022).

[66]G. Bisker, I. A. Martinez, J. M. Horowitz, and J. M. Parrondo, "Comment on" inferring broken detailed balance in the absence of observable currents"", arXiv preprint arXiv:2202.02064 (2022).

[67]J. van der Meer, J. Degünther, and U. Seifert, "Time-resolved statistics of snippets as general framework for model-free entropy estimators", arXiv preprint arXiv:2211.17032 (2022).

[68]J. Ehrich, "Tightest bound on hidden entropy production from partially observed dynamics", Journal of Statistical Mechanics: Theory and Experiment **2021**, 083214 (2021).

[69]D. J. Skinner and J. Dunkel, "Improved bounds on entropy production in living systems", Proceedings of the National Academy of Sciences **118**, e2024300118 (2021).

[70]J. Schnakenberg, "Network theory of microscopic and macroscopic behavior of master equation systems", Reviews of Modern Physics **48**, 571 (1976).

[71]C. Maes, K. Netočnỳ, and B. Wynants, "Dynamical fluctuations for semi-markov processes", Journal of Physics A: Mathematical and Theoretical **42**, 365002 (2009).

[72]J. Zhang and T. Zhou, "Markovian approaches to modeling intracellular reaction processes with molecular memory", Proceedings of the National Academy of Sciences **116**, 23542–23550 (2019).

[73]D. Hartich and A. Godec, "Violation of local detailed balance despite a clear timescale separation", arXiv preprint arXiv:2111.14734 (2021).

[74]D. Hartich and A. Godec, "Comment on" inferring broken detailed balance in the absence of observable currents"", arXiv preprint arXiv:2112.08978 (2021).

[75]Z. Ugray, L. Lasdon, J. Plummer, F. Glover, J. Kelly, and R. Martı, "Scatter search and local nlp solvers: a multistart framework for global optimization", INFORMS Journal on Computing **19**, 328–340 (2007).

[76]J. A. Nirody, A. L. Nord, and R. M. Berry, "Load-dependent adaptation near zero load in the bacterial flagellar motor", Journal of The Royal Society Interface **16**, 20190300 (2019).

[77]T. H. Tan, G. A. Watson, Y.-C. Chao, J. Li, T. R. Gingrich, J. M. Horowitz, and N. Fakhri, "Scale-dependent irreversibility in living matter", arXiv preprint arXiv:2107.05701 (2021).

תקציר

תהליכים מחוץ לשיווי משקל שוברים סימטרייה להיפוך בזמן ומייצרים אנטרופיה. מערכות חיות פועלות רחוק משיווי משקל ברמה המיקרוסקופית של מנועים מולקולריים המנצלים גרדיאנטים של פוטנציאל כימי בכדי להמיר אנרגיה חופשית לעבודה מכנית המלווה בפיזור אנרגיה. כמות האנרגיה שמתפזרת או לחלופין קצב ייצור האנטרופיה מציב הגבלות תרמודינמיות על תהליכים תאיים. בפועל, יש קושי בחישוב קצב ייצור האנטרופיה הנובע ממגבלות ברזולוציה זמנית ומרחבית או מחוסר במידע מלא של חלק מדרגות החופש. בעבודה זאת, אני מציע גישה חדשה לקבלת חסם תחתון הדוק על קצב השינוי באנטרופיה המלא בהינתן מידע חלקי, המתבסס על פתרון של בעיית אופטימיזציה המשתמשת בסטטיסטיקות על המידע של מעברים וזמני המתנה הנראים לעין. אני מציג היררכיה של חסמים המתסמכים על מעברים מסדר ראשון ושני ועל מומנטים של התפלגויות זמני המתנה, ובודק את הגישה שלי על שתי מערכות כלליות, רשת חבויה ומנוע מולקולרי עם מצבים מקובצים. לבסוף, אני מראה שאפשר להשיג חסם תחתון לקצב השינוי באנטרופיה בעזרת הגישה שלי כאשר מניחים שהמערכת המלאה היא בעלת טופולוגיה פשוטה.

בית הספר לפיזיקה ולאסטרונומיה
החוג לפיזיקה של חומר מעובה

חסמים אוניברסליים על קצב יצירת האנטרופיה המחושבים ממידע חלקי

חיבור זה הוגש כחלק מהדרישות לקבלת התואר מוסמך אוניברסיטה
בבית הספר לפיזיקה ואטסרונומיה, אוניברסיטת תל אביב

על ידי

עדן ניצן

העבודה הוכנה בהדרכתה של **דר' גילי ביסקר**